

# Ionic liquids as amphiphile self-assembly media†

Tamar L. Greaves<sup>a</sup> and Calum J. Drummond<sup>\*ab</sup>

Received 11th April 2008

First published as an Advance Article on the web 25th June 2008

DOI: 10.1039/b801395k

In recent years, the number of non-aqueous solvents which mediate hydrocarbon–solvent interactions and promote the self-assembly of amphiphiles has been markedly increased by the reporting of over 30 ionic liquids which possess this previously unusual solvent characteristic. This new situation allows a different exploration of the molecular “solvophobic effect” and tests the current understanding of amphiphile self-assembly. Interestingly, both protic and aprotic ionic liquids support amphiphile self-assembly, indicating that it is not required for the solvents to be able to form a hydrogen bonded network. Here, the use of ionic liquids as amphiphile self-assembly media is reviewed, including micelle and liquid crystalline mesophase formation, their use as a solvent phase in microemulsions and emulsions, and the emerging field of nanostructured inorganic materials synthesis. Surfactants, lipids and block co-polymers are the focus amphiphile classes in this *critical review* (174 references).

## 1. Introduction

Ideal room temperature ionic liquids (ILs) consist solely of ions, and are liquid at temperatures below 100 °C. ILs have been used as solvents in a wide range of applications,<sup>1</sup> including organic synthesis and catalysis,<sup>2–6</sup> inorganic synthesis,<sup>7</sup> chromatography,<sup>8</sup> analytical systems<sup>9,10</sup> and in biological systems.<sup>11</sup> Perhaps their most unique capability is that some ILs possess the ability to support the self-assembly of amphiphiles. Amphiphiles consist of hydrophobic and hydrophilic moieties, and include surfactants, lipids and block copolymers.

We believe the first report of amphiphile self-assembly in a non-aqueous liquid was by Reinsborough and Bloom for the molten salt, pyridinium chloride (melting point 146 °C), where micellisation of cationic surfactants was demonstrated in a series of five papers between 1967 and 1970.<sup>12–16</sup> This ability was first reported for an IL at ambient temperatures in the early 1980s by Evans *et al.* who reported micelle formation in ethylammonium nitrate (EAN).<sup>17,18</sup> There has recently been a very strong renewed interest in this field, with many new ILs reported which can support amphiphile self-assembly.

The ability of some ILs to support the self-assembly of amphiphiles is of particular importance since, other than ILs, there is a very limited number of known solvents possessing this capability. To our knowledge, the first report of amphiphile self-assembly in a non-aqueous solvent at ambient temperature was by Ray in 1969 for ethylene glycol.<sup>19</sup> The effect of different non-aqueous solvents on liquid crystalline mesophase formation has previously been reported for protic solvents such as

<sup>a</sup> CSIRO Molecular and Health Technologies (CMHT), Bag 10, Clayton, VIC 3169, Australia

<sup>b</sup> CSIRO Materials Science and Engineering (CMSE), Private Bag 33, Clayton MDC, VIC 3169, Australia.

E-mail: calum.drummond@csiro.au; Tel: +61 3 9545 2050

† Electronic supplementary information (ESI) available: Additional tables of data. See DOI: 10.1039/b801395k



Tamar L. Greaves

Tamar Greaves obtained her BSc (1995) and PhD (2004) degrees in Physics from Monash University in 2004. Since then she has been a postdoctoral fellow at CSIRO in the Molecular Health and Technologies division, within Prof. Calum Drummond's group.



Calum J. Drummond

Calum Drummond received a PhD in Physical Chemistry from The University of Melbourne in 1987. He is Chief of CSIRO Materials Science and Engineering and an Australian Research Council Federation Fellow at CSIRO Molecular and Health Technologies. Prior to this, he was seconded from CSIRO to be the inaugural Vice President Research at CAP-XX. CAP-XX manufactures electrical double layer capacitors for consumer electronic products. His research interests are in the area of colloid and surface science, including applications of amphiphile self-assembly materials.

formamide,<sup>20–31</sup> *N*-methylformamide,<sup>28</sup> glycerol,<sup>20,26–28</sup> ethylene glycol,<sup>19,27</sup> propylene glycol,<sup>20</sup> butylene glycol,<sup>20</sup> *N*-methylacetamide<sup>21</sup> and hydrazine,<sup>21,31</sup> and the aprotic solvents of *N*-methylsydnone<sup>32</sup> and dimethylformamide.<sup>20,21,28,31</sup> The use of non-aqueous self-assembly solvents was reviewed by Ward and du Reau in 1993.<sup>33</sup> A series of papers has been written by Auvray, Rico and Lattes *et al.* on the behaviour of amphiphiles such as hexadecyltrimethylammonium bromide (CTAB), cetylpyridinium bromide (CPBr) and sodium dodecyl sulfate (SDS) in various polar solvents, including formamide, ethylene glycol, glycerol and *N*-methylformamide.<sup>23–28,32,34–37</sup>

Many new ILs can be created from different cation and anion combinations, which allows the possibility of tailoring self-assembly solvents with specific desired properties. Previously, changing the properties of a self-assembly system was effectively limited to modifying the amphiphile. The use of ILs as self-assembly media readily enables the modification of either the solvent or amphiphile.

The use of ILs as solvents for amphiphile self-assembly was briefly reviewed by Baker and Pandey in 2005,<sup>38</sup> and more recently in another short review by Hao and Zemb, in 2007.<sup>39</sup> The review by Baker and Pandey highlighted how limited the field had been up to 2005, with EAN, BMIm PF<sub>6</sub> and BMIm Cl the only room temperature ILs which were reported as solvents for amphiphile self-assembly.<sup>38</sup> The more recent review by Hao and Zemb highlighted that room temperature ILs can be used as solvents for amphiphile self-assembly into micelles, vesicles and liquid crystals, as solvent phases in microemulsions, and in the preparation of nanoparticles.<sup>39</sup> Significant new work has been reported in this field since these two earlier reviews were published.

Short reviews on the use of ILs in the synthesis of inorganic nanomaterials were given by Zhou in 2005<sup>7</sup> and Antonietti *et al.* in 2004.<sup>40</sup> Since 2005, there has been a growing amount of research devoted to the use of ILs as self-assembly media. There have been many new ILs reported which can support amphiphile self-assembly, a greater range of amphiphile–IL systems characterised, and considerable use of ILs as solvents in the preparation of nanomaterials.

A wide range of ILs have been used as self-assembly media, and the most commonly used cations and anions are represented in Fig. 1 and 2, respectively. There are two broad categories of ILs which are relevant for their use in self-assembly, *viz.* protic ionic liquids (PILs) and aprotic ionic liquids (AILs). The PILs

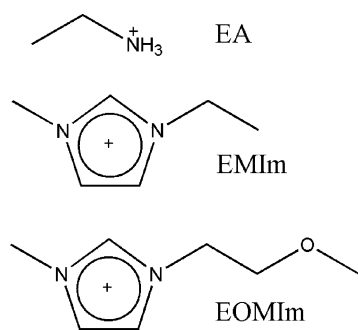


**Fig. 1** Structures of ethylammonium (EA), 1-ethyl-3-methylimidazolium (EMIm) and 1-(2-methoxyethyl)-3-methylimidazolium (EOMIm) cations.

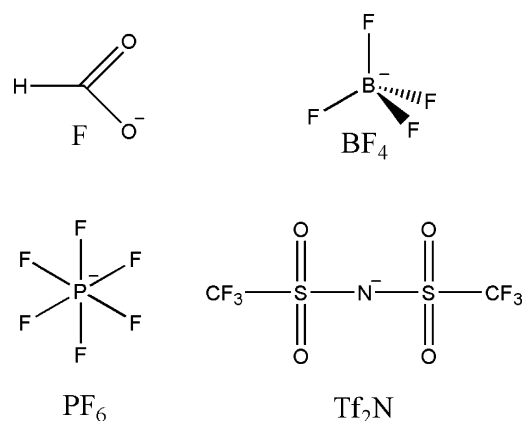


**Fig. 2** Structures of formate (F), tetrafluoroborate (BF<sub>4</sub>), hexafluorophosphate (PF<sub>6</sub>) and bis(trifluoromethanesulfonyl)imide [(CF<sub>3</sub>SO<sub>2</sub>)<sub>2</sub>N] (Tf<sub>2</sub>N) anions.

have the greatest similarity to water due to their protic nature and general solvent properties, such as polarity, with many of the alkylammonium PILs, such as EAN, being capable of supporting self-assembly.<sup>1</sup> The AILs represent the largest number of ILs studied to date, such as the very commonly used di-substituted imidazolium cations such as EMIm, shown in Fig. 1, with a few having been reported to have self-assembly promotion capabilities. Amphiphilic ILs (AmILs) can be either PILs or AILs and they contain a long alkyl chain and are generally used as amphiphiles not solvents. Many AmILs have thermotropic properties, forming liquid crystal phases with no additional solvent present. Thermotropic ILs have been excellently reviewed by Binnemans up to mid 2005.<sup>41</sup>

Despite the vast amount of research conducted into self-assembly, the process is still not fully understood. The ability to utilise different solvents, such as ILs, may aid in advancing the understanding of the self-assembly process, thus potentially providing greater control over it. IL solvent properties and the thermodynamic principles governing the solvent–amphiphile self-assembly process are discussed in the following two sections, with a comparison of ILs to water and non-aqueous solvents.

Most of the publications on ILs as amphiphile self-assembly solvents have been in the past few years. Currently the majority of the work has been on reporting new systems where ILs are behaving as self-assembly solvents, and on the understanding of the mechanisms. More recently, applications have been developed to utilise ILs as self-assembly solvents in the synthesis of nanostructured materials.

This review focuses on the use of ILs as non-aqueous self-assembly media up to early 2008. Pertinent properties of ILs are covered first, followed by the formation of micelles, lyotropic liquid crystal phases, microemulsions, emulsions and nanoparticles in ILs. The uses of AmILs as amphiphiles in aqueous or other non-IL solvents have not been included. Thermotropic ILs are briefly discussed. A strong emphasis has been placed on an examination of ILs as self-assembly solvents compared to water.

## 2. Ionic liquid solvent properties

The solvent properties of PILs<sup>1</sup> and AILs<sup>42</sup> have generally been described in the literature for specific applications, such

as for chromatography,<sup>8</sup> electrochemistry,<sup>43</sup> or organic synthesis.<sup>4</sup> However, both PILs and AILs are tailorable solvents in that they can be designed to have specific physicochemical properties through structural changes in the cation or anion. Consequently, properties such as viscosity, conductivity, density and surface tension of ILs cover a broad range of values and cannot be generalised, though typically the viscosities of ILs are greater than water.

To date, a wide range of PILs, and a small number of AILs, have been reported which are capable of supporting amphiphile self-assembly. The main differences between these two classes of ILs are that the PILs are capable of donating and accepting hydrogen bonds, and hence can form hydrogen bonded networks similar to water, whereas AILs cannot.

The formation of PILs occurs through proton transfer from a Brønsted acid to a Brønsted base. Ideally this transfer is complete, with only fully ionised species present. However, it is speculated that many PILs contain some of the molecular acid and base precursor species, though there are difficulties in establishing the proportions.<sup>1,44,45</sup> In contrast, most AILs are usually assumed to be fully ionised, though there may be a degree of complexation. ILs are frequently described in the literature as having non-negligible vapour pressures, though this is not universally true, with many PILs having significant vapour pressures (which enables some of them to be distillable).

The ionic species present in the PILs and AILs may undergo some degree of association. One method of estimating the degree of association was proposed by Kohler *et al.*,<sup>46</sup> and has been used to show that typically there is less association in AILs than PILs.<sup>1</sup>

### 3. Specific self-assembly connected properties of ionic liquids compared to water and non-aqueous non-ionic solvents

The self-assembly of amphiphiles in water is generally considered to be governed by the hydrophobic effect, which has been the subject of numerous papers, and has been covered well by recent reviews.<sup>47–49</sup> From this perspective the formation of the simplest aggregates, micelles, and more complex aggregate structures is governed by the interplay of the entropy and enthalpy terms in the free energy of aggregation, as given in eqn (1), where  $\Delta G^\circ_{\text{agg}}$  is the free energy associated with aggregation,  $\Delta H^\circ_{\text{agg}}$  is the enthalpy change,  $T$  the temperature and  $\Delta S^\circ_{\text{agg}}$  the change in entropy. Alternatively,  $\Delta G^\circ_{\text{agg}}$  can be directly related to the critical aggregation concentration, CAC, as in eqn (2).

$$\Delta G^\circ_{\text{agg}} = \Delta H^\circ_{\text{agg}} - T\Delta S^\circ_{\text{agg}} \quad (1)$$

$$\Delta G^\circ_{\text{agg}} = -RT \ln(\text{CAC}) \quad (2)$$

At ambient temperature, the hydrophobic effect, and formation of aggregates, is mainly entropy driven, with a large negative entropy contribution to the free energy on transfer of hydrocarbon moieties into the aggregate interior. The temperature has a significant effect, with, for example, increasing temperature causing the entropy term to decrease such that near the boiling point of water the entropy contribution to the free energy becomes positive and hence is no longer a driving

force for aggregation.<sup>33,48</sup> Other significant factors may include van der Waals, hydrogen bonding and electrostatic interactions which make the aggregation of amphiphiles in water, or other solvents, complex. The  $\Delta G^\circ_{\text{agg}}$  for charged amphiphiles is also regularly represented<sup>50,51</sup> as the sum of the contributions from hydrophobic,  $\Delta G_{\text{hc}}$ , and electrostatic,  $\Delta G_{\text{el}}$ , interactions, with

$$\Delta G^\circ_{\text{agg}} = \Delta G_{\text{hc}} + \Delta G_{\text{el}} \quad (3)$$

In ionic liquids, the surface charge screening from the ionic media will lead to the electrostatic term,  $\Delta G_{\text{el}}$ , in eqn (3) becoming negligible, such that  $\Delta G^\circ_{\text{agg}} \approx \Delta G_{\text{hc}}$ .

The first report of micelle formation in non-aqueous solvents at room temperature was by Ray in 1969,<sup>19</sup> with later work by Ray<sup>20</sup> emphasising that the hydrophobic effect was not limited to water, but was part of a larger solvophobic effect. Most of the literature on non-aqueous self-assembly media from the early 1970s to 1993 was reviewed by Ward and du Reau.<sup>33</sup> A more recent paper by Akhter and Alawi in 2003 compares micelle formation in formamide, *N*-methylformamide and *N,N*-dimethylformamide.<sup>31</sup>

Studies of the thermodynamic driving force for the aggregation of amphiphiles in ILs have been nearly exclusively based on EAN, with the majority conducted by Evans *et al.* in the 1980s.<sup>17,18,52,53</sup> The interest in EAN arose after it was shown to be capable of supporting amphiphile micelle formation. The free energy of micellisation is analogous to that of the transfer of nonpolar gases into water.<sup>53</sup>

The free energy, enthalpy and entropy associated with the transfer of nonpolar gases into EAN or water are very similar, indicating that the solvophobic force in EAN is similar to the hydrophobic force in water, and is dominated by the entropic contribution. Direct force measurements between large surfaces indicate that EAN exhibits a macroscopic “solvophobic effect” similar to that observed for water.<sup>54</sup> The transfer process for nonpolar gases is more energetically favourable in EAN than in water, showing the higher affinity of EAN for hydrophobic groups compared to water. The thermodynamic values for the transfer of nonpolar gases into EAN or water are provided in Table S1 of the ESI†.

A thermodynamic consideration of transferring nonpolar gases to EAN indicated that EAN has “water-like” properties. However, the transfer of alcohols to EAN showed that the heat capacity behaviour was not similar for EAN and water.<sup>55</sup> At the time, this difference was attributed to EAN not having fluctuations between different isomeric states which cold water was stated as having. Mirejovsky and Arnett found EAN to be more similar to other non-aqueous polar solvents such as DMF, NMF, DMSO, and ethylene glycol than like water.<sup>55</sup>

The free energy associated with the transfer of a methylene ( $-\text{CH}_2-$ ) group from the EAN to the interior of a micelle was calculated by Evans *et al.* to be either  $-370$  or  $-420$  cal mol<sup>-1</sup> at 50 °C (depending on what method was used to calculate the value), compared to  $-680$  cal mol<sup>-1</sup> in water.<sup>17</sup> It was suggested by Evans *et al.* that the large positive entropy in water and EAN on micellisation was due to the breaking of structure from around the hydrocarbon chain when it was transferred into the micelle.<sup>17</sup>

The lower free energy for transfer of methylene groups from the solvent to a micelle interior in EAN than water means it is more energetically favourable for hydrocarbon groups to be exposed to solvent in EAN than in water. This strongly affects the preferred structure of the amphiphile–EAN systems compared to water, since structures with more hydrocarbon chains exposed will be more stable, and more energetically favourable in EAN than in water.<sup>18</sup> Consistent with this, phospholipid aggregate structures have been reported to have a preference for more curved structures such as micellar or inverse hexagonal,<sup>56,57</sup> requiring longer amphiphile chains in order to observe micelle to lamellar transitions under similar conditions to water.<sup>56</sup>

The majority of the relevant thermodynamic information reported has been for EAN. However, the enthalpies of gel to bilayer transitions of dialkyldimethylammonium amphiphiles in ether containing imidazolium ILs have been reported by Kimizuka and Nakashima, and Tang *et al.* (see section 7).<sup>58–60</sup> The phase transitions occurred at much higher temperatures than in water, with enthalpy and entropy values about half as large as when water was the solvent.<sup>59</sup>

#### 4. Solvent cohesion, self-assembly and the Gordon parameter

The driving force for amphiphile self-assembly in solvents was discussed by Evans<sup>53</sup> with reference to the Gordon parameter,  $G$ , as given by eqn (4), where  $\gamma$  is the air–liquid surface tension and  $V_m$  is the molar volume. The Gordon parameter gives a measure of the cohesive energy density of the solvent, with higher  $G$  values suggesting a stronger driving force for the self-assembly process.

$$G = \gamma/V_m^{-1/3} \quad (4)$$

The Gordon values for the ILs discussed in this review paper are given in Table 1, and for comparison water and other non-aqueous solvents capable of supporting amphiphile self-assembly have been included. Currently the solvent with the lowest known Gordon value which is capable of supporting amphiphile self-assembly is the PIL ethylammonium butyrate (EAB), with  $G = 0.576 \text{ J m}^{-3}$ .<sup>61</sup> It should be noted that the AILs that are currently known to promote amphiphile self-assembly have higher  $G$  values than EAB.

A key observation with PILs has been that higher  $G$  values tend to be linked to greater liquid crystalline phase diversity and larger bands of thermal stability.<sup>61–63</sup> Consequently, the design of ILs as rich self-assembly media should take into consideration structural features which are likely to lead to increased  $G$  values through increasing the surface tension, or decreasing the molar volume.

Similarly, it has been reported by Auvray *et al.* that there is a strong relationship between the solvophobic interaction strength of protic solvents, as shown by their cohesive energy density, and the mesophase diversity observed for different amphiphiles. Further details can be found in the series of papers by Auvray *et al.*, such as in ref. 28.

**Table 1** Gordon parameters of ILs used as self-assembly media for amphiphiles. For comparison, water and three non-aqueous molecular self-assembly media have been included

Solvent	Gordon value/ $\text{J m}^{-3}$
Water	$\sim 2.8$ , <sup>53</sup> 2.743, <sup>62</sup> 2.75 <sup>64</sup>
Formamide	1.50 <sup>64</sup>
Ethylene glycol	1.20 <sup>64</sup>
Glycerol	1.51
EMIm Tf <sub>2</sub> N	0.613 <sup>a</sup> , <sup>65,66</sup>
BMIm PF <sub>6</sub> <sup>+</sup>	0.822 <sup>a</sup> , <sup>67</sup> 0.790 <sup>a</sup> , <sup>68</sup>
BMIm BF <sub>4</sub> <sup>+</sup>	0.794 <sup>a</sup> , <sup>67</sup>
MAF	1.041 <sup>b</sup> , <sup>61</sup>
EAF	0.867 <sup>b</sup> , <sup>61</sup>
BAF	0.669 <sup>b</sup> , <sup>61</sup>
PeAF	0.614 <sup>b</sup> , <sup>61</sup>
2MPAF	0.629 <sup>b</sup> , <sup>61</sup>
2MBAF	0.596 <sup>b</sup> , <sup>61</sup>
EOAF	1.448 <sup>b</sup> , <sup>61</sup>
2POAF	0.977 <sup>b</sup> , <sup>61</sup>
EOAA	1.099 <sup>b</sup> , <sup>61</sup>
EAP	0.644 <sup>b</sup> , <sup>61</sup>
EAB	0.576 <sup>b</sup> , <sup>61</sup>
EAG	1.056 <sup>b</sup> , <sup>61</sup>
EAL	0.793 <sup>b</sup> , <sup>61</sup>
EOAL	1.149 <sup>b</sup> , <sup>61</sup>
EAN	1.060 <sup>b</sup> , <sup>61</sup> 1.40 <sup>64</sup> , 1.3 <sup>53</sup>
EOAN	1.097 <sup>b</sup> , <sup>61</sup>
EAHS	1.215 <sup>b</sup> , <sup>61</sup>
DEAF	0.775 <sup>a</sup> , <sup>63</sup>
TEAF	0.812 <sup>a</sup> , <sup>63</sup>
DEOAF	1.185 <sup>a</sup> , <sup>63</sup>
DMAF	0.997 <sup>a</sup> , <sup>63</sup>
DMAHS	1.540 <sup>a</sup> , <sup>63</sup>
EOAHS	1.698 <sup>a</sup> , <sup>63</sup>
2MEAF	0.891 <sup>a</sup> , <sup>63</sup>
22HEEAF	1.032 <sup>a</sup> , <sup>63</sup>
22HEEAN	1.223 <sup>a</sup> , <sup>63</sup>

<sup>a</sup> Value at 25 °C. <sup>b</sup> Value at 27 °C.

#### 5. Self-assembled aggregate structure and the critical packing parameter (CPP)

Given that the free energy for aggregation is favourable, the liquid crystalline mesophases which form for a specific amphiphile–solvent system are dependent upon many factors. These can be generalised into the amphiphile geometry and interactions of the amphiphile with the solvent, and the effect that increasing the concentration has on the aggregate packing density.

A powerful and simple tool for developing a first-order understanding of mesophase formation is the critical packing parameter (CPP), as given in eqn (5) where  $v$  is the average volume of the amphiphile,  $a$  is the effective head group area and  $l$  is the effective chain length of the amphiphile in its molten state.<sup>69</sup> The liquid crystalline mesophases are represented in Fig. 3, with the CPP increasing from left to right, with spherical micelles for  $\text{CPP} < 1/3$ , rod shaped micelles for  $1/3 < \text{CPP} < 1/2$ , bilayers and vesicles for  $1/2 < \text{CPP} < 1$  and inverted structures when  $\text{CPP} > 1$ .

$$\text{CPP} = v/al \quad (5)$$

Amphiphiles can be geometrically represented as shown in Fig. 4, according to whether their CPP is less than, equal to or greater than 1. Without taking aggregate packing density into

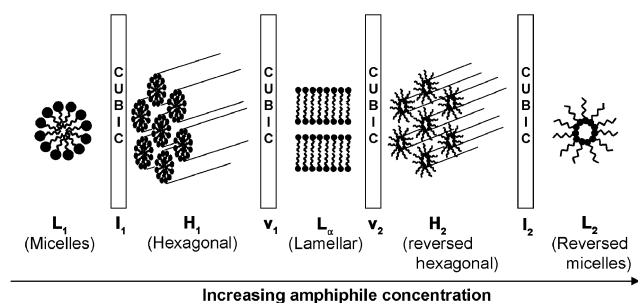


**Fig. 3** Generalised scheme for liquid crystal mesophases observed as a function of amphiphile concentration. (From ref. 70 – Reproduced by permission of the PCCP Ownership Board). Note that the term ‘reversed’ in the figure is equivalent to the term ‘inverse’ used throughout this review paper.

account, the effective molecular shape of each amphiphile will lead to a preferred CPP, and hence preferred liquid crystalline mesophase. The amphiphile represented in Fig. 4a has  $CPP < 1$  and hence a preference for normal phases, such as the  $L_1$ ,  $I_1$ ,  $H_1$  or  $V_1$  phases shown in Fig. 3. The amphiphile in Fig. 4b has  $CPP = 1$ , and a preference for a  $L_\alpha$  phase, while the amphiphile in Fig. 4c has  $CPP > 1$  and a preference for inverted structures, such as  $V_2$ ,  $H_2$ ,  $I_2$  or  $L_2$  shown in Fig. 3.

In addition to the effective molecular shape of the amphiphile, the amphiphile concentration, or packing density has a critical role in controlling the liquid crystalline mesophase. The phase progression shown in Fig. 3 corresponds to the ideal phase progression from left to right for increasing amphiphile concentration, as the phases with higher CPP enable greater proportions of amphiphiles to be accommodated.

An excellent summary of the relationship between CPP, the hydrocarbon volume fraction and the main liquid crystalline mesophases is given in Fig. 5, reproduced from Hyde.<sup>71</sup> Increasing the amphiphile concentration generally corresponds to moving towards the top right of the diagram in Fig. 5, since the additional amphiphile usually increases the apolar volume fraction along with the greater packing density as CPP is increased.

The use of ILs as amphiphile self-assembly solvents in comparison to water, or other molecular solvents, will have some inherent differences. The high ionic strength of the ILs

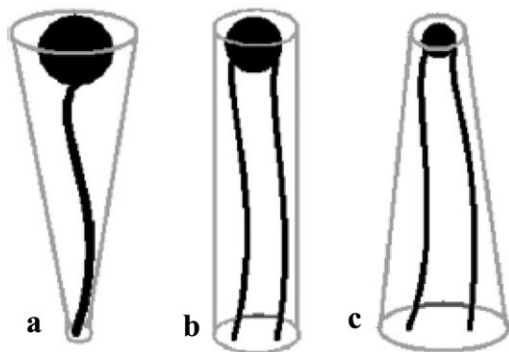


**Fig. 4** Representation of amphiphiles with (a)  $CPP < 1$ , (b)  $CPP = 1$ , and (c)  $CPP > 1$ . (From ref. 70 – Reproduced by permission of the PCCP Ownership Board).

will screen the headgroup charge for anionic and cationic surfactants,<sup>50,51,72</sup> leading to a decrease in the effective  $a$  of the surfactants in ILs compared to in water.

In aqueous systems, the presence of electrolytes have been shown to influence the counter-ion dissociation of cationic surfactants, such as CTAB.<sup>50,51,72</sup> In ILs, a similar effect is envisaged, along with ion exchange of the counter ion with the ions of the IL.

A further complexity is that ILs can behave as co-surfactants, leading to a decrease in the charge per unit area for charged amphiphiles, and an increase in the effective  $v$  for all amphiphiles. The effect of co-surfactants has been investigated in water systems, such as 1-pentanol in cationic dodecyltrimethylammonium halide micelles,<sup>73</sup> where increasing the 1-pentanol concentration led to less energetically favourable interactions between the micellar headgroups and the counter ions.

## 6. Micelle formation in ionic liquids

In mixtures of amphiphiles and water, the amphiphiles will organise themselves to minimise the free energy of the system. The driving force for this structural orientation is the minimisation of the contact of the hydrocarbon regions of the amphiphiles with the polar solvent. The critical micelle concentration (CMC) is the minimum concentration of amphiphiles required at a given temperature for micelles to form. Below this concentration the amphiphiles are present as free monomers in solution, and at the air–liquid interface with the hydrocarbon region orientated away from the solution. At the CMC there is spontaneous formation of micelles.

Depending on the amphiphile concentration, either normal or inverse micelles can form. Normal micelles have a continuous water phase, with the polar headgroups of the amphiphiles pointing towards the bulk solvent and the amphiphile hydrocarbon chains pointing towards the micelle interior. For inverse micelles, the amphiphiles have the polar headgroup towards the micelle interior and an aqueous core.

As an initial point of reference, the micellisation process in ILs can be considered with reference to the process in water. In water, the process is spontaneous, with frequently a very clear discontinuity in the solution properties as a function of concentration at the CMC, reflecting the single step of monomer  $\leftrightarrow n$ -mer. Similarly, Evans *et al.* observed that in EAN there was a sharp discontinuity in many of the solvent properties, suggesting a similar spontaneous micelle formation process, as in water, and not a step-wise aggregation process.<sup>17</sup> There has been insufficient data reported to determine whether the micellisation process is always spontaneous in ILs. The molten salt pyridinium chloride was reported by Reinsborough *et al.* in the late 1960s to support the formation of micelles, and to have a clearly defined CMC, suggesting a spontaneous process in this salt.<sup>12–16</sup> In the review paper by Ward and du Reau in 1993, it was suggested based on the poorly defined CMC that micelles form in polar non-aqueous media through a stepwise aggregation process, from monomer  $\leftrightarrow$  dimer  $\leftrightarrow$  trimer  $\leftrightarrow n$ -mer.<sup>33</sup> Other observed differences for polar non-aqueous media compared to water have been higher Krafft temperatures for ionic surfactants, where the Krafft temperature is the

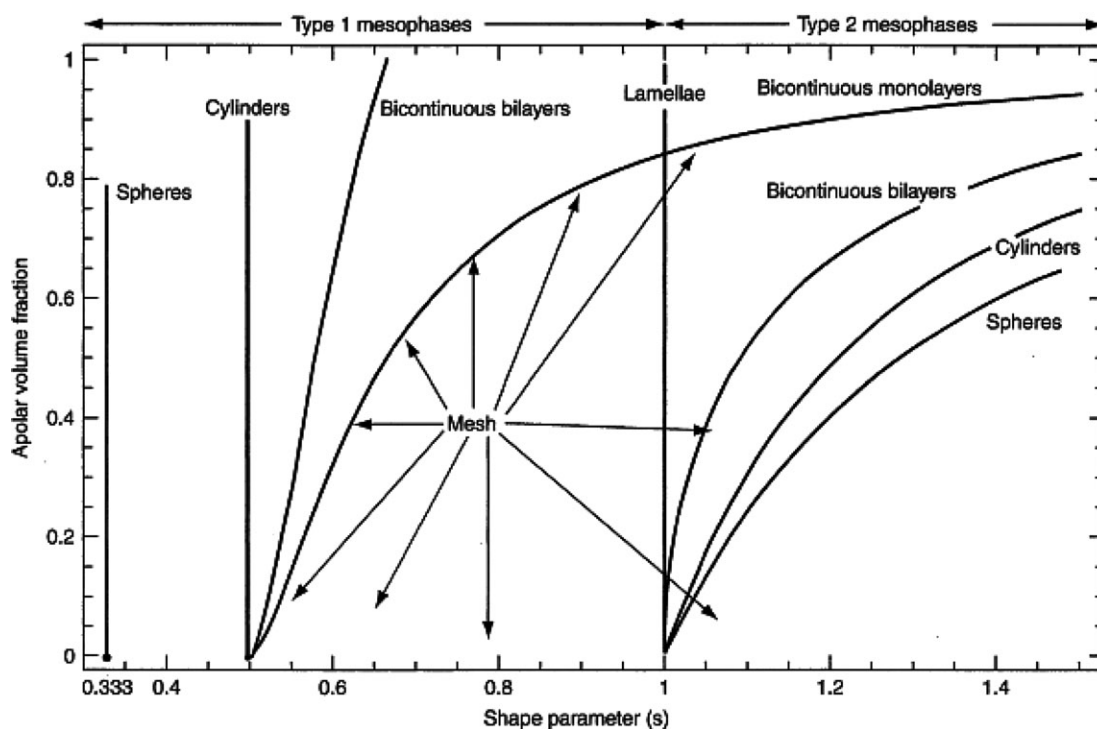


**Fig. 5** General lyotropic phase diagram, relating CPP (denoted shape parameter ( $s$ ) in figure), hydrocarbon volume (apolar volume fraction) and the mesophases. (Reproduced from ref. 71 with permission. Copyright 2001, John Wiley and Sons).

minimum temperature at which micelles form, smaller micelles, and a greater variety in geometries compared to the situation where there are spherical micelles in water.<sup>33</sup>

As far as we can ascertain, CMC measurements have only been reported for amphiphiles in the ILs EAN, BMIm Cl, BMIm PF<sub>6</sub> and EMIm TFSA. The CMCs for cationic, anionic and non-ionic amphiphiles in these ILs are listed in Table 2, along with the corresponding CMCs in water, where available. The structures of these amphiphiles are shown in Fig. 6, along with others relevant to later sections of this paper.

The work in the early 1980s by Evans *et al.* using EAN provided an excellent comparison between EAN and water,<sup>18</sup> showing that these two solvents shared many similarities, which were described in section 3 on specific self-assembly connected properties of ionic liquids. The driving force for amphiphile aggregation in EAN appears to be similar to that in water, in that it appears to be due to the entropy gain from the transfer of the hydrocarbon out of the EAN.<sup>17</sup> One of the main differences between EAN and water is that hydrocarbons are more soluble in EAN than in water, and hence there is a weaker driving force for them to form micelles. This leads to higher CMCs in EAN, since there is greater solubility of the amphiphiles in EAN, and the finding that longer amphiphiles are required in EAN to observe similar aggregation behaviour to that in water.<sup>85–87</sup> The CMC of CTAB in EAN compared with other solvents is given in Table 3. Unfortunately values could not be obtained for the list at a consistent temperature. The CMC of CTAB in EAN or water was about mid range for these solvents. Unlike in water, the nitrate anion present in EAN can compete with the bromide counterion in CTAB.

In contrast to water, it was shown by Velasco *et al.* in 2006 that the formation of micelles of alkylammonium nitrate amphiphiles in EAN did not cause a change in the partial molar volume of EAN. In water, the formation of micelles causes the partial molar volume to increase, and the lack of change in EAN suggests that the micellisation process in EAN does not significantly change the solvent structure.<sup>79</sup>

The aggregation of the amphiphilic ILs (AmILs) C<sub>16</sub>MIm Cl and C<sub>16</sub>MImBF<sub>4</sub> in EAN was recently reported by Kunz and Thomaier,<sup>82</sup> with the assumption that the structures formed were micelles. The critical aggregation concentrations (CAC) for these systems are given in Table 2, along with the analogous water systems. The AmILs in water had CACs which were comparable to the CMC of common cationic amphiphiles such as CTAB. In contrast, the AmILs in EAN were a factor of 10 greater, which was consistent with other amphiphiles in EAN compared to water.<sup>82</sup> Preliminary results have indicated that these aggregate systems of AmILs in ILs may be stable at temperatures greater than 200 °C, though possibly only briefly.<sup>82</sup>

The use of AILs as self-assembly media is a very new field, with, to our knowledge, the first report made by Anderson *et al.* in 2003 on the formation of micelles in BMIm Cl and BMIm PF<sub>6</sub>,<sup>80</sup> closely followed by Fletcher and Pandey using the AIL EMIm Tf<sub>2</sub>N.<sup>76</sup> Unlike the PIL EAN, these AILs have considerable differences in their solvent properties compared to water, such as being unable to form hydrogen bonded networks.

A series of non-ionic alkyl poly(ethylene oxide) amphiphiles in BMIm BF<sub>4</sub>, BMIm PF<sub>6</sub> and BMIm Tf<sub>2</sub>N was reported by de Lauth-Vigurie *et al.* in 2006.<sup>83</sup> It was assumed that micelles

**Table 2** Critical micelle concentrations (CMC) of amphiphiles in ionic liquids compared to aqueous and non-aqueous solvents at the noted temperatures

Surfactant	Solvent	Temp./ °C	CMC/M
C <sub>12</sub> TAB	EAN	50	0.023 <sup>a</sup> 17
	Water	25	0.01534 <sup>74</sup>
		30	0.01563 <sup>75</sup>
C <sub>14</sub> TAB	EAN	50	0.00697 <sup>a</sup> 17
	Water	25	0.003943 <sup>74</sup>
		30	0.00375 <sup>75</sup>
CTAB	EAN	50	0.00223 <sup>a</sup> 17
	EMIm Tf <sub>2</sub> N	25	No aggregation <sup>76</sup>
		Water	25
C <sub>14</sub> PyrB	EAN	30	9.1 × 10 <sup>-4</sup> 75
		25	0.097 <sup>b</sup> 18
	Water	25	0.00649 <sup>a</sup> 17
C <sub>16</sub> PyrB	EAN	50	0.0027 <sup>77</sup>
		30	0.00337 <sup>b</sup> 78
	Water	25	0.00169 <sup>a</sup> 17
C <sub>18</sub> PyrB	EAN	50	0.020 <sup>b</sup> 18
		30	6.4 × 10 <sup>-4</sup> 77
	Water	25	8.8162 × 10 <sup>-4</sup> b 78
C <sub>5</sub> AN	Formamide	30	7.1 × 10 <sup>-4</sup> 75
		25	0.075 <sup>28</sup>
	EAN	50	5.69 × 10 <sup>-4</sup> a 17
C <sub>8</sub> AN	EAN	25	0.35 <sup>79</sup>
C <sub>10</sub> AN	EAN	25	0.079 <sup>79</sup>
C <sub>12</sub> AN	EAN	25	0.025 <sup>79</sup>
SDS	EAN	25	0.0079 <sup>79</sup>
		25	0.048 <sup>80</sup>
	BMIm Cl	c	Did not dissolve <sup>76</sup>
Brij 35	EMIm Tf <sub>2</sub> N	c	8 × 10 <sup>-3</sup> 80
		c	0.115, <sup>80</sup> 0.108 ± 0.009 <sup>81</sup>
	Water	c	0.060 ± 0.006 <sup>81</sup>
Brij 700	EMIm Tf <sub>2</sub> N	25	~0.05 <sup>76</sup>
		c	1.6 × 10 <sup>-3</sup> 80
	Water	c	(0.06–0.09) × 10 <sup>-3</sup> 80
Triton X-100	BMIm PF <sub>6</sub>	c	0.020 <sup>80</sup>
		c	0.021 ± 0.015 <sup>81</sup>
	EMIm Tf <sub>2</sub> N	c	0.017 ± 0.002 <sup>81</sup>
Tween-20	EMIm Tf <sub>2</sub> N	25	~0.01 <sup>76</sup>
		c	5.93 × 10 <sup>-3</sup> a 17
	Water	c	6.11 × 10 <sup>-3</sup> a 17
docSS	EMIm Tf <sub>2</sub> N	c	0.113 ± 0.019 <sup>81</sup>
		c	>0.10 <sup>76</sup>
	Water	c	0.0002 <sup>d</sup> 81
SB3-10	EMIm Tf <sub>2</sub> N	25	0.070 ± 0.002 <sup>81</sup>
		c	~0.05 <sup>76</sup>
	Water	c	0.00008 <sup>81</sup>
OBG	BMIm Cl	c	4.7 × 10 <sup>-3</sup> 80
		c	9.1 × 10 <sup>-4</sup> 80
	Water	c	0.29 <sup>80</sup>
C <sub>16</sub> MimCl	BMIm PF <sub>6</sub>	c	0.466 <sup>80</sup>
		c	0.377 ± 0.09 <sup>81</sup>
	Water	c	0.029 <sup>80</sup>
C <sub>16</sub> MImBF <sub>4</sub>	EMIm Tf <sub>2</sub> N	c	0.108 ± 0.009 <sup>81</sup>
		c	0.024 <sup>d</sup> 81
	Water	c	0.0162 <sup>e</sup> 82
C <sub>16</sub> E <sub>8</sub>	EAN	40	8.88 × 10 <sup>-4</sup> e 82
		40	0.0136 <sup>e</sup> 82
	Water	40	1.37 × 10 <sup>-3</sup> e 82
C <sub>14</sub> E <sub>8</sub>	BMIm BF <sub>4</sub>	25	(9 ± 1) × 10 <sup>-3</sup> 83
		25	0.0005 × 10 <sup>-3</sup> f 83
	Formamide	25	11 × 10 <sup>-3</sup> f 83
C <sub>12</sub> E <sub>8</sub>	BMIm PF <sub>6</sub>	25	(27 ± 1) × 10 <sup>-3</sup> 83
		25	(76 ± 3) × 10 <sup>-3</sup> 83
	Water	25	g 83
Phytantriol	BMIm Tf <sub>2</sub> N	25	0.009 × 10 <sup>-3</sup> f 83
		25	(93 ± 2) × 10 <sup>-3</sup> 83
	Formamide	25	0.1 × 10 <sup>-3</sup> f 83
Phytantriol	BMIm BF <sub>4</sub>	25	8.1 × 10 <sup>-5</sup> 84
		25	35 × 10 <sup>-3</sup> f 83

**Table 2 (continued)**

Surfactant	Solvent	Temp./ °C	CMC/M
C <sub>12</sub> E <sub>6</sub>	BMIm BF <sub>4</sub>	25	(57 ± 2) × 10 <sup>-3</sup> 83
		25	6.7 × 10 <sup>-5</sup> f 83
	Formamide	25	31 × 10 <sup>-3</sup> f 83
C <sub>12</sub> E <sub>4</sub>	BMIm BF <sub>4</sub>	25	(46 ± 1) × 10 <sup>-3</sup> 83
		25	0.065 × 10 <sup>-3</sup> f 83
	Formamide	25	25 × 10 <sup>-3</sup> f 83

<sup>a</sup> CMC given as mole fraction. <sup>b</sup> CMC as mol kg<sup>-1</sup>. <sup>c</sup> Temperature unlisted, probably RT. <sup>d</sup> Data from a reference within this reference. <sup>e</sup> Critical aggregation concentration (CAC). <sup>f</sup> From a reference within this reference. <sup>g</sup> No aggregation observed.

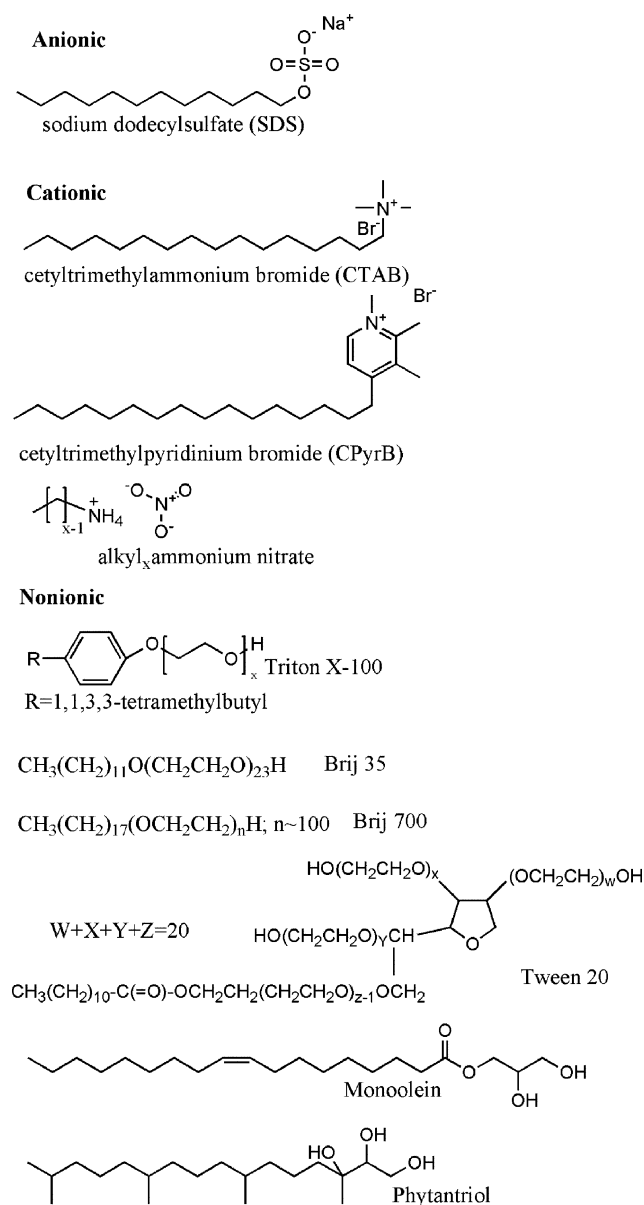


**Fig. 6** Molecular structures of many of the amphiphiles studied in ILs.

**Table 3** CMC of the amphiphile CTAB in different solvents

Solvent	Temp./°C	CMC/M
Water	25	$9.642 \times 10^{-4}$ <sup>a 74</sup>
	25	$9.0 \times 10^{-4}$ <sup>a 21</sup>
	30	$9.1 \times 10^{-4}$ <sup>75</sup>
	50	$1.05 \times 10^{-3}$ <sup>75</sup>
	50	$2.23 \times 10^{-3}$ <sup>b 17</sup>
EAN	50	No aggregation <sup>76</sup>
EMIm Tf <sub>2</sub> N	25	$7.41 \times 10^{-4}$ <sup>21</sup>
Formamide	25	0.09 <sup>22</sup>
	60	0.14 <sup>22</sup>
Ethylene glycol	60	No aggregation <sup>21</sup>
<i>N</i> -Methylformamide	20–55	$9.07 \times 10^{-3}$ <sup>21</sup>
<i>N,N'</i> -Dimethylformamide	25	$7.46 \times 10^{-5}$ <sup>21</sup>
<i>N</i> -Methylacetamide	30	No aggregation <sup>21</sup>
<i>N,N'</i> -Dimethylacetamide	20–55	$3.540 \times 10^{-3}$ <sup>21</sup>
Dimethyl sulfoxide	35	

<sup>a</sup> Metastable as 25 °C is below the Krafft temperature of CTAB in water. <sup>b</sup> CMC given as mole fraction.

had formed in BMIm BF<sub>4</sub> and BMIm PF<sub>6</sub> based on the change in surface tension with concentration. No change in surface tension as a function of concentration was detected for BMIm Tf<sub>2</sub>N. The CMCs for the amphiphile–IL systems are given in Table 2, and the aggregation numbers and hydrodynamic radii in Table S2 of the ESI†. The aggregation numbers were estimated from conductivity as a function of concentration,<sup>75</sup> through fitting the Szyszkowski–Langmuir equation,<sup>83</sup> or by extrapolating the Debye plot to zero concentration.<sup>18</sup> The hydrodynamic radii were calculated using the Stokes–Einstein equation<sup>18,82</sup> or from dynamic light scattering (DLS) experiments.<sup>83</sup>

The reported CMCs in the ILs were significantly higher than in water. An investigation was conducted by Sarkar *et al.* into the solution dynamics of two of these systems, *viz.* micellar solutions of C<sub>12</sub>E<sub>8</sub> and C<sub>14</sub>E<sub>8</sub> in BMIm BF<sub>4</sub>.<sup>88</sup>

The formation of micelles of diblock and triblock copolymers in the ILs BMIm PF<sub>6</sub> and EMIm Tf<sub>2</sub>N was reported by Lodge *et al.*<sup>89–93</sup> Representative cryo-TEM images of the micelles are shown in Fig. 7a, and the worm-like micelles and vesicles in Fig. 7b. The diblock copolymers used were poly((1,2-butadiene)-*block*-ethylene oxide) (PB-PEO)<sup>89</sup> and polystyrene-*block*-poly(methyl methacrylate) (PS-PMMA),<sup>91</sup> and the triblock copolymers were poly(styrene-*block*-ethylene oxide-*block*-styrene) (SOS)<sup>92</sup> and poly(*N*-isopropyl acryla-

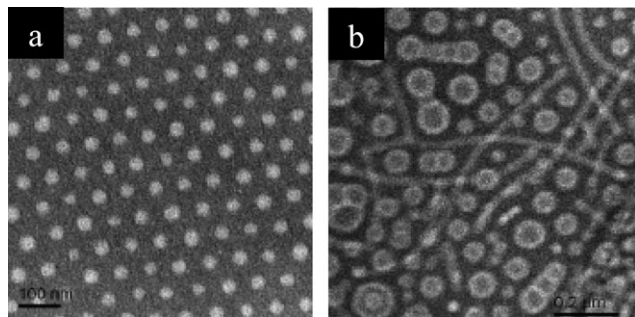


**Fig. 7** Cryo-TEM images of (a) micelles of 1 wt% block copolymer BO(9-20) in BMIm PF<sub>6</sub>, (b) worm-like micelles and vesicles of 1 wt% block copolymer BO(9-4) in BMIm PF<sub>6</sub>. (Reproduced from ref. 89 with permission. Copyright 2006, American Chemical Society).

mid-*block*-ethylene oxide-*block*-*N*-isopropyl acrylamide) (PNIPAm-PEO-PNIPAm).<sup>93</sup> BMIm PF<sub>6</sub> was shown to have similar solvent properties towards the block copolymers as water, and was a good solvent for the PEO and PMMA blocks, and a non-solvent for the PB, PS and PNIPAm blocks. In contrast to other IL–amphiphile systems, it appears that there may be a stronger driving force for self-assembly of the PB-PEO block copolymer in BMIm PF<sub>6</sub> than in water, due to a greater interfacial tension between the soluble and non-soluble polymer components in the IL.<sup>89</sup> The composition of the block copolymers were varied, and led to the same sequence of micelle structures in the IL that is seen in water, progressing from spheres to wormlike micelles and then to bilayered vesicles.<sup>89,91</sup>

To date there has been limited reporting of aggregation numbers and radii for micelles in ILs. The data suggest that micelles in EAN are much smaller than in water, such that the hydrocarbon chains must be somewhat folded to fit inside the micelles.<sup>18</sup> Smaller micelles are able to form in EAN compared to water, since hydrocarbons are more soluble in EAN, and hence can tolerate the greater exposure of hydrocarbon resulting from the smaller micelles.<sup>18</sup> The non-ionic C<sub>*n*</sub>E<sub>*m*</sub> amphiphiles in BMIm BF<sub>4</sub> and BMIm PF<sub>6</sub> had smaller aggregation numbers than in water, and smaller hydrodynamic radii.<sup>83</sup> The aggregation numbers of the amphiphiles Brij 35, docSS, SDS and SB3-10 in BMIm PF<sub>6</sub> and BMIm Cl were large,<sup>80</sup> such that there was too much scattering to determine their size using small-angle neutron scattering (SANS). Clearly, the understanding of what governs micellar size and shape in ILs is still evolving.

## 7. Liquid crystalline mesophase formation in ionic liquids

The first report of amphiphile self-assembly in ILs to create non-micellar aggregates was in 1983 by Evans *et al.* on the formation of phospholipid mesophases in EAN<sup>85</sup> and this system was the focus of a number of studies from that time until 1992.<sup>56,57,94,95</sup>

A tabulated summary of the phospholipid mesophases reported in the literature is given in Table S3 of the ESI†. It is evident that there were fewer phase transitions observed in EAN. Generally the phase progressions were similar in EAN and in water, except for the high temperature phases which were always lamellar in water, but usually non-lamellar in EAN. This has been attributed to a preference of the phospholipids towards curved surfaces, due to the higher solubility of hydrocarbons in EAN compared to water allowing greater contact between the hydrocarbon and EAN.

More recently, IL–amphiphile systems have been reported which are capable of supporting all the main lyotropic liquid crystalline mesophases in EAN,<sup>61,62,86</sup> other protic ILs<sup>61–63</sup> and in aprotic imidazolium ILs.<sup>58,60,96</sup> A summary of the liquid crystal mesophases for IL–amphiphile systems reported in the literature is given in Table 4. The water–amphiphile lyotropic phase behaviour has been included where available, along with the phase behaviour of CTAB in different polar self-assembly media. It is evident from Table 4 that all the main mesophases have been observed, consisting of discrete



**Table 4** Temperature ranges over which liquid crystalline mesophases have been observed for amphiphiles in ionic liquids. Water and other non-aqueous solvents have been included for comparison. Temperatures in °C

IL	Surfactant	I <sub>1</sub>	H <sub>1</sub>	V <sub>1</sub>	L <sub>α</sub>	V <sub>2</sub>	H <sub>2</sub>	T <sub>C</sub>
EAN	C <sub>14</sub> E <sub>4</sub>				~ < 50 <sup>a</sup> 86			49 <sup>86</sup>
EAN	C <sub>14</sub> E <sub>8</sub>		~ < 30 <sup>a</sup> 86					
EAN	C <sub>16</sub> E <sub>4</sub>				> 60 <sup>a</sup> 86			88 <sup>86</sup>
Water	C <sub>16</sub> E <sub>6</sub>		34 <sup>97</sup>	34 <sup>97</sup>	< 102 <sup>97</sup>			37 <sup>97</sup>
EAN	C <sub>16</sub> E <sub>6</sub>	< 40 <sup>a</sup> 86	< 67 <sup>a</sup> 86	< 48 <sup>a</sup> 86				130 <sup>86</sup>
Water	C <sub>16</sub> E <sub>8</sub>	12 <sup>97</sup>	58 <sup>97</sup>	62 <sup>97</sup>	~ < 106 <sup>97</sup>			63 <sup>97</sup>
EAN	C <sub>16</sub> E <sub>8</sub>		< 60 <sup>a</sup> 86					
EAN	C <sub>18</sub> E <sub>2</sub>				> 50 <sup>a</sup> 86			74 <sup>86</sup>
EAN	C <sub>18</sub> E <sub>4</sub>				> 50 <sup>a</sup> 86			105 <sup>86</sup>
EAN	C <sub>18</sub> E <sub>6</sub>	~ < 35 <sup>a</sup> 86	< 60 <sup>a</sup> 86	< 56 <sup>a</sup> 86	< 96 <sup>a</sup> 86			123 <sup>86</sup>
EAN	C <sub>18</sub> E <sub>8</sub>	~ < 40 <sup>a</sup> 86	< 60 <sup>a</sup> 86	< 45–50 <sup>a</sup> 86	55–60 <sup>a</sup> 86			
Water	CTAB		25–190 <sup>97</sup>	40–185 <sup>97</sup>	50–> 200 <sup>97</sup>			
Glycerol	CTAB		55–> 150 <sup>98</sup>	75–135 <sup>98</sup>	80–> 150 <sup>98</sup>			
Formamide	CTAB		50–125 <sup>99</sup>		75–> 150 <sup>99</sup>			
Ethylene glycol	CTAB		55–90 <sup>98</sup>	75–85 <sup>98</sup>	80–> 100 <sup>98</sup>			
MAF	CTAB		71–90 <sup>61</sup>	72–91 <sup>61</sup>	79–85 <sup>61</sup>			
EAF	CTAB				84–98 <sup>61</sup>			
PAF	CTAB				89–> 98 <sup>61</sup>			
BAF	CTAB				80–97 <sup>61</sup>			
PeAF	CTAB				78–> 100 <sup>61</sup>			
2MPAF	CTAB				66–74 <sup>61</sup>			
2MBAF	CTAB				88–> 103 <sup>61</sup>			
3MBAF	CTAB				84–> 104 <sup>61</sup>			
EOAF	CTAB		73–> 105 <sup>61</sup>	82–> 105 <sup>61</sup>	92–105 <sup>61</sup>			
2POAF	CTAB		67–> 99 <sup>61</sup>	82–> 106 <sup>61</sup>	97–104 <sup>61</sup>			
EAA	CTAB				91–> 98 <sup>61</sup>			
EOAA	CTAB		82–93 <sup>61</sup>	86–91 <sup>61</sup>	93–> 99 <sup>61</sup>			
EAP	CTAB				68–> 98 <sup>61</sup>			
EAB	CTAB				80–90 <sup>61</sup>			
EAG	CTAB		82–101 <sup>61</sup>	92–101 <sup>61</sup>	94–94 <sup>61</sup>			
EAL	CTAB		65–> 100 <sup>61</sup>	80–> 100 <sup>61</sup>	82–92 <sup>61</sup>			
EOAL	CTAB		66–100 <sup>61</sup>	76–> 100 <sup>61</sup>	76–91 <sup>61</sup>			
EAN	CTAB		58–> 104 <sup>61</sup>	76–104 <sup>61</sup>	76–90 <sup>61</sup>			
EOAN	CTAB		69–96 <sup>61</sup>	75–> 98 <sup>61</sup>	78–96 <sup>61</sup>			
EAHS	CTAB		64–> 101 <sup>61</sup>	80–> 98 <sup>61</sup>	83–98 <sup>61</sup>			
DMAF	CTAB				88–> 107 <sup>63</sup>			
DEAF	CTAB				98–> 104 <sup>63</sup>			
DEOAF	CTAB		70–> 107 <sup>63</sup>	88–> 107 <sup>63</sup>	88–> 107 <sup>63</sup>			
2MEAF	CTAB			91–104 <sup>63</sup>	88–104 <sup>63</sup>			
22HEEAF	CTAB				83–> 106 <sup>63</sup>			
22HEEAN	CTAB		71–> 106 <sup>63</sup>	78–106 <sup>63</sup>	82–> 106 <sup>63</sup>			
DMAHS <sup>b</sup>	CTAB		67–> 107 <sup>63</sup>					
EOAHS <sup>b</sup>	CTAB		54–> 105 <sup>63</sup>					
EATFA	CTAB				88–> 106 <sup>63</sup>			
TEOAF	CTAB		79–96 <sup>63</sup>	89–96 <sup>63</sup>	92–> 124 <sup>63</sup>			
2MEAN	CTAB		74–> 106 <sup>63</sup>	80–106 <sup>63</sup>	81–102 <sup>63</sup>			
DEOAN	CTAB		73–> 107 <sup>63</sup>	88–107 <sup>63</sup>	87–> 107 <sup>63</sup>			
TEOAN	CTAB		114–> 132 <sup>63</sup>	116–132 <sup>63</sup>				
MATFA <sup>b</sup>	CTAB			94–> 108 <sup>63</sup>	83–> 108 <sup>63</sup>			
Water	Myverol				27–> 50 <sup>100</sup> , 20–86 <sup>c</sup> 101	20–> 50 <sup>100</sup> , 20–48 <sup>c</sup> 101	84–98 <sup>c</sup> 101	
MAF	Myverol				23–44 <sup>62</sup>	23–44 <sup>62</sup>		
EAF	Myverol				23–56 <sup>62</sup>	23–40 <sup>62</sup>		
PAF	Myverol				24–58 <sup>62</sup>	25–36 <sup>62</sup>		
BAF	Myverol						23–41 <sup>62</sup>	
PeAF	Myverol						23–42 <sup>62</sup>	
3MBAF <sup>b</sup>	Myverol				24–41 <sup>62</sup>			
EOAF <sup>b</sup>	Myverol					22–50 <sup>62</sup>	23–88 <sup>62</sup>	
2POAF	Myverol				18–92 <sup>62</sup>			
EOAA	Myverol				24–70 <sup>62</sup>	32–59 <sup>62</sup>		
EAP	Myverol						25–41 <sup>62</sup>	
EAG	Myverol				18–39 <sup>62</sup>	18–39 <sup>62</sup>		
EAL	Myverol				< 24–49 <sup>62</sup>	34–54 <sup>62</sup>		
EOAL	Myverol				< 23–71 <sup>62</sup>	36–54 <sup>62</sup>		
EAN	Myverol				< 22–88 <sup>62</sup>			
EOAN	Myverol						23–73 <sup>62</sup>	
EAHS <sup>b</sup>	Myverol					23–52 <sup>62</sup>	23–64 <sup>62</sup>	
DMAF	Myverol				17–43 <sup>63</sup>			
DEOAF	Myverol				22–61 <sup>63</sup>	31–63 <sup>63</sup>		
2MEAF	Myverol				22–35 <sup>63</sup>			
22HEEAF	Myverol				8–47 <sup>63</sup>	26–59 <sup>63</sup>		

Table 4 (continued)

IL	Surfactant	I <sub>1</sub>	H <sub>1</sub>	V <sub>1</sub>	L <sub>α</sub>	V <sub>2</sub>	H <sub>2</sub>	T <sub>C</sub>
22HEEAN <sup>b</sup>	Myverol				23–42 <sup>63</sup>	28–47 <sup>63</sup>		
DMAHS	Myverol						22–51 <sup>63</sup>	
EOAHS	Myverol						24–52 <sup>63</sup>	
2MEAN	Myverol				37–46 <sup>63</sup>			
Water	Phytantriol				22–35 <sup>102</sup>	22–48 <sup>102</sup>	44–60 <sup>102</sup>	
MAF	Phytantriol				15–53 <sup>62</sup>			
EAF	Phytantriol				9–36 <sup>62</sup>			
PAF <sup>b</sup>	Phytantriol				24–38 <sup>62</sup>			
BAF	Phytantriol						18–35 <sup>62</sup>	
PeAF <sup>b</sup>	Phytantriol						26–54 <sup>62</sup>	
2MPAF	Phytantriol						12–28 <sup>62</sup>	
2MBAF <sup>b</sup>	Phytantriol				16–23 <sup>62</sup>			
3MBAF	Phytantriol						20–34 <sup>62</sup>	
EOAF	Phytantriol				16–51 <sup>62</sup>	25–42 <sup>62</sup>		
2POAF	Phytantriol				16–63 <sup>62</sup>			
EOAA	Phytantriol				18–56 <sup>62</sup>			
EAP <sup>b</sup>	Phytantriol				11–34 <sup>62</sup>			
EAB	Phytantriol						12–26 <sup>62</sup>	
EAG	Phytantriol					23–58 <sup>62</sup>	23–67 <sup>62</sup>	
EAL <sup>b</sup>	Phytantriol				8–25 <sup>62</sup>			
EOAL <sup>d</sup>	Phytantriol				13–38 <sup>62</sup>			
EAN	Phytantriol				22–65 <sup>62</sup>	35–60 <sup>62</sup>		
EOAN	Phytantriol						23–43 <sup>62</sup>	
EAHS	Phytantriol				22–33 <sup>62</sup>	22–33 <sup>62</sup>		
DMAF	Phytantriol				4–18 <sup>63</sup>			
DEAF <sup>b</sup>	Phytantriol				4–22 <sup>63</sup>			
DEOAF	Phytantriol				8–42 <sup>63</sup>	28–42 <sup>63</sup>		
2MEAF <sup>b</sup>	Phytantriol				10–31 <sup>63</sup>			
22HEEAF	Phytantriol						8–17 <sup>63</sup>	
22HEEAN	Phytantriol						6–20 <sup>63</sup>	
DMAHS	Phytantriol						13–43 <sup>63</sup>	
EOAHS	Phytantriol						10–79 <sup>63</sup>	
2MEAN	Phytantriol				37–41 <sup>63</sup>			
BMI <sub>m</sub> PF <sub>6</sub>	P123		<25–>65 <sup>e</sup> 96		<25–>65 <sup>f</sup> 96			
BMI <sub>m</sub> BF <sub>4</sub>	Brij 76				<sup>d</sup> 60			110 <sup>60</sup>
EOMI <sub>m</sub> Br	DADMA <sub>12</sub>				>52 <sup>g</sup> 59			
MOMI <sub>m</sub> Br	DADMA <sub>12</sub>				>51 <sup>g</sup> 59			
EOMI <sub>m</sub> Br	DADMA <sub>14</sub>				>72 <sup>g</sup> 59			
MOMI <sub>m</sub> Br	DADMA <sub>14</sub>				>71 <sup>g</sup> 59			
EOMI <sub>m</sub> Br	Glycolipid 1				>47 <sup>h</sup> 58			
MOMI <sub>m</sub> Br	Glycolipid 1				>43 <sup>h</sup> 58			
EOMI <sub>m</sub> Br	Glycolipid 2				>40 <sup>i</sup> 58			
MOMI <sub>m</sub> Br	Glycolipid 2				>51 <sup>i</sup> 58			

<sup>a</sup> Maximum temperature where this phase was present. <sup>b</sup> Some phase ambiguity reported in paper. <sup>c</sup> Phases for monoolein, which is the main constituent of myverol 18-99K. <sup>d</sup> Self-assembled aggregates observed were nanofibers, gel and vesicles. <sup>e</sup> Hexagonal phase present at 25 °C for concentrations of P123 from 40–50%. <sup>f</sup> Lamellar phase present at 25 °C for concentrations of P123 from 68–85%. <sup>g</sup> 10 mM of the cationic amphiphile in the IL. Bilayer membrane. Mentioned in reference that there were microcrystalline aggregates formed at room temperature, perhaps multilayered bilayers, which transformed into vesicles above the phase transition temperature. <sup>h</sup> 10 mM of the cationic amphiphile in the IL. Bilayer membrane. <sup>i</sup> 10 mM of the cationic amphiphile in the IL. Fibrous nanostructure at room temperature, and vesicles above phase transition temperature.

cubic, I<sub>1</sub>, normal hexagonal, H<sub>1</sub>, normal bicontinuous cubic, V<sub>1</sub>, lamellar, L<sub>α</sub>, inverse bicontinuous cubic, V<sub>2</sub>, inverse hexagonal, H<sub>2</sub>, inverse discrete cubic, I<sub>2</sub>, and inverse micellar, L<sub>2</sub>. The phases were either identified by employing cross-polarised optical microscopy (POM),<sup>60–63,86,96</sup> or by using SAXS.<sup>96</sup> Representative liquid crystal phase textures of the IL–amphiphile systems are shown in Fig. 8.

The solvophobic interaction between PILs and amphiphiles is considered to be similar to water and amphiphiles or other polar self-assembly media. Like water, the PILs are good solvents for the polar regions of the amphiphiles, and poor solvents for the apolar regions. For the AILs which are not capable of forming hydrogen bonds, the solvophobic interaction is based on the AILs being good solvents for the polar

regions and poor solvents for the apolar regions of the amphiphiles. This solvent behaviour drives the self-assembly process to minimise the solvent contact with the apolar regions. The lyotropic liquid crystal phase progressions in the ILs with increasing concentration and/or temperature were comparable to what occurs in water (represented in Fig. 3), which can be seen from Table 4; though often there were fewer phases observed in the ILs.

The phase behaviour of non-ionic polyoxyethylene alkyl ether surfactants, described by C<sub>n</sub>E<sub>m</sub>, in EAN was shown by Araos and Warr to be very similar to the analogous water systems.<sup>86</sup> Longer amphiphile chains were required in EAN to obtain the same thermal ranges and phases as in the water systems, and for example the C<sub>16</sub>E<sub>6</sub>–EAN system compared

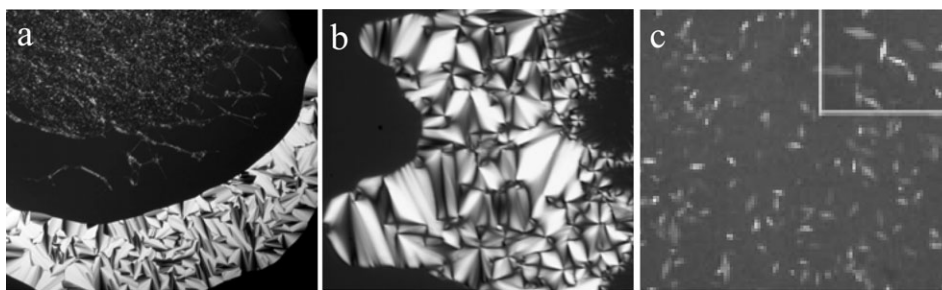


**Fig. 8** Representative liquid crystalline mesophase textures of amphiphiles in ILs under cross-polarised optical microscopy. (a) CTAB in 2-propanolammonium formate at 97 °C showing hexagonal, isotropic cubic and lamellar phases, with neat CTAB in the top left corner. (Reproduced from ref. 61 with permission. Copyright 2007, American Chemical Society). (b) Myverol 18-99K, predominately monoolein, in ethylammonium propionate at 31 °C showing inverse hexagonal phase texture, with neat myverol on the right. (Reproduced from ref. 62 with permission. Copyright 2007, American Chemical Society). (c) 45 wt% of Pluronic P123 in BMIm PF<sub>6</sub> showing an anisotropic phase (determined by SAXS to be lamellar). (From ref. 96–Reproduced by permission of The Royal Society of Chemistry).

well to the C<sub>12</sub>E<sub>8</sub>–water system.<sup>86</sup> The same phase progressions were observed with increasing amphiphile concentration of discrete cubic, hexagonal, bicontinuous cubic then lamellar. Systematic changes to the amphiphile alkyl and ethylene oxide chain lengths led to similar trends in the phases in EAN and water.<sup>86</sup> Phase diagrams for C<sub>16</sub>E<sub>6</sub>–EAN and C<sub>18</sub>E<sub>6</sub>–EAN<sup>86</sup> were reported based on flooding experiments of liquid penetration into neat amphiphile.

The phase behaviour of polybutadiene-polyethylene oxide (PB-PEO) diblock copolymers in EMIm Tf<sub>2</sub>N and BMIm PF<sub>6</sub> was shown by Lodge and Simone to be similar to the behaviour in water at 25 °C.<sup>90</sup> All the same phases were detected in the ILs as in water, though there were much greater regions on the phase diagrams of coexisting microstructures in the ILs than in water.<sup>90</sup>

Screening studies were conducted by Greaves *et al.* on the lyotropic phase behaviour of amphiphiles in a series of protic ILs, as shown in Table 4.<sup>61–63</sup> The ILs consisted of primary, secondary or tertiary ammonium cations with simple carboxylate or inorganic anions. The amphiphiles were the cationic CTAB and the non-ionic myverol 18-99K (primarily monoolein) and phytantriol. These investigations were unusual in that changes to the mesophases as a result of varying the structure of the solvent, and not the amphiphile, were determined. This highlighted that ILs are tailorable solvents for self-assembly, where either the amphiphile or solvent could be modified to achieve desired amphiphile self-assembly structures.

The same phases and phase progressions occurred in the PILs and water of normal hexagonal, lamellar, inverse bicontinuous cubic and inverse hexagonal phases.<sup>61–63</sup> The PIL–CTAB and water–CTAB systems were fairly similar, though fewer phases were present in some of the PILs. In the PIL–myverol 18-99K and PIL–phytantriol systems, there were more differences compared to water. As can be seen from Table 4, the onset of the inverse hexagonal phase was at low to ambient temperatures in the PILs, compared to 84 °C for water–myverol 18-99K or 44 °C for water–phytantriol. It appears that the inverse hexagonal and lamellar phases were competing over the same concentration and thermal range, and hence either inverse hexagonal or lamellar phases were observed in the PILs but not both.

Gordon parameter, *G*, values were generally related to the phase behaviour, with high *G* values a good indication of a strong driving force for self-assembly, as shown by greater phase diversity and thermal ranges.<sup>61–63</sup> However, it is only an indication, and other structural features and properties are important.<sup>63</sup> Trends were identified relating the PIL structure and *G* value to the mesophases, such as hydroxyl groups and short alkyl chains leading to higher *G* values and an increased likelihood for cubic phases to form.

Increasing the alkyl chain length of the PILs led to lower *G* values and a greater tendency for them to be co-surfactants. As co-surfactants, the PILs increased the CPP, through increasing the hydrocarbon volume, *v*, leading to a preference for the higher curvature inverse hexagonal phase compared to the lamellar phase. This can be seen for the series MAF, EAF, PAF, BAF, PeAF with myverol 18-99K or phytantriol.

In contrast to water, and other molecular solvents capable of supporting amphiphile self-assembly, ILs consist of cations and anions, and hence can undergo ion exchange with surfactants, particularly anion exchange with cationic surfactants.

The alkyl chains present on the cations or anions of the ILs lead to their partitioning into the amphiphile–IL interface and behaving as co-surfactants. The longer the alkyl chain, the greater the effect.<sup>61–63</sup> ILs containing long alkyl chains (greater than 5 methylene groups) become amphiphilic in nature, and are not discussed in this review.

There have been few investigations into the formation of liquid crystalline mesophases in aprotic ILs. A preliminary study was conducted by Tang *et al.* using the non-ionic amphiphile Brij 76 in BMIm BF<sub>4</sub>, as listed in Table 4.<sup>60</sup> A tentative liquid crystal phase progression was proposed of nanofibers to gel to vesicles. As part of an investigation into the use of ILs as solvents for cellulose, it was briefly mentioned that solutions containing >10% cellulose in BMIm Cl led to the formation of liquid crystal phases.<sup>103</sup> These phases were detected as optically anisotropic using cross-polarised microscopy, though no information was given about the phases.

The amphiphilic block copolymer of P123 (EO<sub>20</sub>PO<sub>70</sub>EO<sub>20</sub>) was reported to form hexagonal and lamellar phases in BMIm PF<sub>6</sub>, as recorded in Table 4.<sup>96</sup> The liquid crystal phases observed occurred at the same concentration ranges in the IL as in water–P123 systems. It was concluded that the

solvophobic interaction was similar to water, in that the IL was a good solvent for the polar EO blocks, and a poor solvent for the apolar PO blocks, which led to the formation of polar and apolar domains.<sup>96</sup> The lattice spacings of the LC phases were smaller in BMIm PF<sub>6</sub> than in water, which was attributed to the higher density of the IL, and different phase textures were observed under crossed-polarised microscopy for the two solvents.

The commonly used aprotic ILs of BMIm BF<sub>4</sub> and BMIm PF<sub>6</sub> were successfully used as solvents to self-assemble the amphiphile Zn(OOCH<sub>2</sub>C<sub>6</sub>F<sub>13</sub>)<sub>2</sub> into bilayer vesicles, which were nanospheres with diameters from 30–90 nm.<sup>104</sup> Similarly, these ILs were used to self-assemble mixtures of Zn(OOCH<sub>2</sub>C<sub>6</sub>F<sub>13</sub>)<sub>2</sub> and C<sub>14</sub>DMAO, which gave different phase behaviour to that observed with just the zinc amphiphile. In both systems, the vesicles had a lamellar structure. In the analogous study in water, the zinc amphiphile alone did not display any self-assembly, indicating a significant difference in the solvophobic interactions between these ILs and water.<sup>104</sup>

Kimizuka and Nakashima have developed ether containing aprotic ILs, which are capable of dissolving some carbohydrates, and enable certain glycolipids and dialkyldimethylammonium cations to self-assemble, with the thermal transitions given in Table 4.<sup>58,59</sup> The water content of the ether-containing ILs was quite high, at 2.4–2.5 wt%, though as a control Kimizuka and Nakashima trialled BMIm PF<sub>6</sub> with similar levels of water present, and no carbohydrate dissolved and self-assembly did not take place.<sup>58</sup> These amphiphiles mostly formed microcrystalline aggregates with bilayer structure, with many undergoing a reversible transition with increased temperature into vesicles. One of the glycolipids, denoted Glycolipid 2 in Table 4, formed a fibrous nanostructured gel at room temperature, and vesicles above the phase transition.<sup>58</sup>

In related work, Yoshio *et al.* have used EMIm BF<sub>4</sub> and EMIm PF<sub>6</sub> as solvents with amphiphilic ILs with thermotropic capabilities. A variety of smectic phases were observed for these systems, however, the ILs should be considered as solvents and not as self-assembly media, since their role is to modify the thermotropic phase behaviour of the amphiphilic ILs.<sup>105,106</sup>

The behaviour of ILs as amphiphile self-assembly solvents appears to have more similarities to protic non-aqueous solvents than to water. In particular, the ILs, like other non-aqueous protic solvents, frequently lead to far less complex phase diagrams than water.<sup>25</sup>

## 8. Microemulsions containing ionic liquids

Conventionally microemulsions contain water and a nonpolar phase stabilised by an amphiphile. Depending on the proportions of the three components the aggregate structures can be water-in-oil, bicontinuous or oil-in-water. The first non-aqueous microemulsions were reported in 1984.<sup>36</sup> Rico and Lattes reported a microemulsion in 1984 containing formamide instead of water,<sup>36</sup> with similar systems reported since then by the same group.<sup>23,25,107</sup> Similarly, in 1984 Friberg and Podzimek reported a microemulsion containing ethylene glycol instead of water.<sup>108</sup>

Analogous behaviour and phases have been observed for microemulsions containing an IL as one of the solvent phases. A review of water-in-oil microemulsions and their use in the synthesis of nanoparticles has been given by Eastoe *et al.* in 2006.<sup>109</sup> Microemulsions containing ILs are of interest due to the potential to expand the solvating abilities of the neat IL, such as improving the solubility of apolar solutes through having hydrophobic domains for oil-in-IL dispersions. Some other solvent applications which have been identified for these microemulsions are as solvents for chemical reactions, in the synthesis of organic or inorganic materials, preparation of nanomaterials, in biological extractions or as solvents for enzymatic reactions.

A tabulated summary of the microemulsions containing an IL as a solvent phase is provided in Table S4 of the ESI†, including for completeness the use of ILs as surfactants to make a microemulsion of water in hexanol.<sup>110</sup> The use of the ILs as surfactants is not utilising their ability to promote the self-assembly of amphiphiles and hence is not further discussed in this review. The majority of studies on IL microemulsions have been conducted by Han *et al.* and Zheng *et al.* using BMIm PF<sub>6</sub>, the non-ionic amphiphile TX-100 and either a non-polar second solvent or water.<sup>111–119</sup>

The first use of an IL as a solvent phase in a microemulsion was reported by Han *et al.* for BMIm BF<sub>4</sub> with Triton X-100 (TX-100) and cyclohexane.<sup>111</sup> This system was later looked at by Eastoe *et al.*,<sup>120</sup> and Sarkar *et al.*<sup>121</sup> Zheng *et al.* used freeze fracture electron microscopy to characterise the size and shape of the aggregates. Previous to this, a microemulsion was prepared by Chang in 1990 using a molten salt mixture of ethylenediamine, ammonia and potassium as one solvent.<sup>122</sup> In this microemulsion, the second solvent phase was decane, with SDS used as a surfactant, and the effect of 1-pentanol on the microemulsion was explored.<sup>122</sup>

From 2004, the groups of Zheng *et al.* and Han *et al.* have reported on the microemulsions formed using the ionic liquid of either BMIm BF<sub>4</sub> or BMIm PF<sub>6</sub>, mostly the surfactant Triton X-100 (TX-100) and a range of non-polar solvents or water as the second solvent phase. There was a particular focus on the characterisation of the microemulsions, including phase diagrams, and development of reliable characterisation techniques. The polarity, solvent properties and formation mechanisms were explored using probe molecules with FTIR, <sup>1</sup>H NMR and UV-Vis spectroscopy. The size and size distribution of the aggregates in the microemulsion were characterised using dynamic light scattering (DLS).

The main phases of interest to Zheng *et al.* and Han *et al.* were the IL-in-oil when the second solvent was a hydrocarbon, or water-in-IL, when the second solvent was water. For IL-in-oil phases, the radius of the aggregates was observed to linearly increase with an increasing proportion of IL,<sup>111,113,115</sup> and similarly for increasing water proportions for water-in-IL emulsions.<sup>112</sup> This was good confirmation that the IL (or water) was in the core, and hence additional IL caused the aggregates to expand, and was consistent with what is seen in conventional aqueous systems.

The phase diagrams of the IL microemulsion systems explored by Zheng *et al.* and Han *et al.* were included in the papers<sup>111–118,123</sup> and a typical phase diagram has been

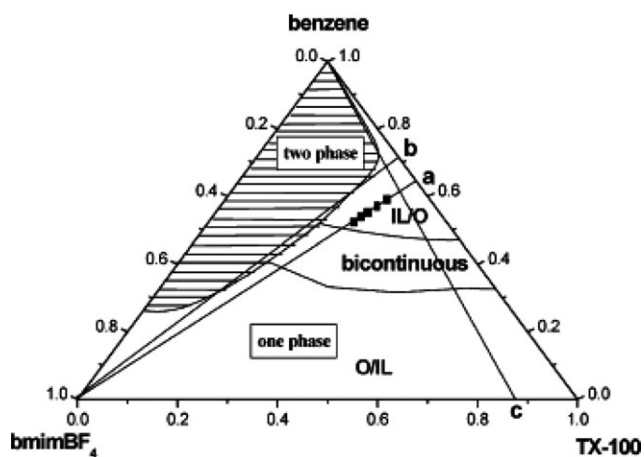


**Fig. 9** Typical phase diagram for a microemulsion containing an IL. The system contains BMIm BF<sub>4</sub>, TX-100 and benzene. (Reproduced from ref. 118 with permission. Copyright 2007, American Chemical Society).

reproduced in Fig. 9 for IL, TX-100 and a nonpolar solvent microemulsion.<sup>117</sup> The single and biphasic regions for the phase diagrams were identified through changing compositions using titration and observing where the solutions were clear (single phase) or turbid (two phases). The single phase region was further divided into IL-in-solvent, bicontinuous and solvent-in-IL using either electrical conductivity measurements<sup>111,113–115,117,118</sup> or diffusion coefficients from cyclic voltammetry experiments.<sup>112,114,116</sup> These two methods gave comparable results,<sup>114</sup> with clearer phase distinction using cyclic voltammetry.

The ILs in the microemulsions containing TX-100 were suggested to be good solvents for the ethylene oxide (EO) groups in TX-100. FTIR and <sup>1</sup>H NMR spectroscopy with probe molecules showed there was a good interaction between the electron density of the EO and the electropositive imidazolium ring on the IL cation.<sup>115</sup>

Using small angle neutron scattering (SANS) it appears that the IL-in-oil aggregates were oblate in shape. The size of the aggregates, as determined by DLS, were typically between 60–150 nm, depending on the specific system and the proportion of IL,<sup>119</sup> which was higher than the aggregate size of less than 40 nm for reversed micelles of water in TX-100.<sup>124</sup> The greater size of the aggregates has been attributed to the larger size of the IL than water, leading to lower curvature and hence larger aggregate size.<sup>115</sup> In contrast, Eastoe *et al.* used SANS to determine the droplet sizes for BMIm BF<sub>4</sub> in cyclohexane and found that they were ellipsoid and between 19–24 Å, with the size increasing as the IL concentration increased.<sup>120</sup> It was mentioned that the light scattering method used by Zheng *et al.* is not reliable, and that they believed the droplet sizes reported by Zheng *et al.* were too large for microemulsions.

It was recently reported by Zheng *et al.* that small additions of water helped stabilise the microemulsion containing BMIm BF<sub>4</sub>, TX-100 and benzene.<sup>117</sup> It was proposed that the stabilisation resulted from the water decreasing the attractive interactions between droplets, with a hydrogen bonded network forming which includes the water, IL cation and anion, and the TX-100 polar region.<sup>118</sup> The water was determined by

FTIR and DLS to be mostly present as bound or trapped water in the interface region.<sup>117,118</sup>

The microemulsions containing BMIm PF<sub>6</sub> and water as the two solvents with either TX-100 or Tween 20 as the surfactant were developed by Han *et al.* as a solvent system for solutes not soluble in the IL but which were soluble in the water domains.<sup>112,116</sup> The phase diagrams for these two systems were different to the one shown in Fig. 9 in that the biphasic region was larger than the single phase regions, though otherwise they were fairly similar. Riboflavin was used as a test biological solute and K<sub>3</sub>Fe(CN)<sub>6</sub> as a test metal salt, where both were insoluble in BMIm PF<sub>6</sub>. These solutes were mostly soluble in the water region of the water-in-IL phase, highlighting the potential use of microemulsions in solvent applications.<sup>116</sup>

The non-aqueous microemulsion of ethylene glycol, TX-100 and BMIm PF<sub>6</sub> was recently reported by Han *et al.*<sup>123</sup> This microemulsion was compared to the analogous microemulsion containing water instead of ethylene glycol to investigate the driving force and mechanism for the formation of the microemulsion.

Microemulsions containing ILs were investigated by Sarkar *et al.* using the probe molecules Coumarin 153 (C-153) and Coumarin 151 (C-151), which are a rigid hydrophobic probe and a flexible hydrophilic probe, respectively.<sup>121,125</sup> The solvent dynamics and rotational relaxation of the probe molecules was observed in the IL-in-oil microemulsion of BMIm BF<sub>4</sub>/TX-100/cyclohexane, and the IL-in-water and water-in-IL microemulsions containing BMIm PF<sub>6</sub>/TX-100/water.<sup>121,125,126</sup> The hydrophobic C-153 in BMIm BF<sub>4</sub>/TX-100/cyclohexane was observed to slowly diffuse into the IL core, whereas C-153 was probably located at the water-IL interface in BMIm PF<sub>6</sub>/TX-100/water.<sup>121,126</sup> The hydrophilic C-151 diffused very slowly into the IL core for BMIm PF<sub>6</sub>/TX-100/water, but otherwise was located at the interface.<sup>126</sup> BMIm PF<sub>6</sub> displayed slower solvation when confined inside the aggregate core compared to bulk IL, which was attributed to slower dynamics within the core.<sup>126</sup> However, this was reported to be a smaller effect than has been seen for most solvents in microemulsions.<sup>121</sup>

In contrast, Pandey *et al.* recently investigated the effect of adding BMIm PF<sub>6</sub> into a micellar system of TX-100 in water, and inferred that the IL partitions into the TX-100 micellar phase, without forming a microemulsion.<sup>127</sup> This is in contrast to Han *et al.* and Sarkar *et al.* who both investigated this system and reported it as a microemulsion.<sup>112,126</sup> At this stage, it remains unclear whether the water/TX-100/BMIm PF<sub>6</sub> system, and hence other analogous microemulsions, are best considered as microemulsions or as modified micellar phases.

The first report of an IL-in-IL microemulsion was made by Han *et al.* in 2007.<sup>128</sup> The microemulsion contained BMIm PF<sub>6</sub> dispersed in PAF with the anionic amphiphile sodium bis(2-ethylhexyl) sulfosuccinate (AOT).

Recently in 2007, Warr and Atkin have reported on microemulsions containing EAN as the polar phase with dodecane as the apolar phase (or other alkanes), along with C<sub>n</sub>E<sub>m</sub> surfactants.<sup>129</sup> In comparison to aqueous systems, higher surfactant concentrations and longer amphiphile apolar chains were required to achieve similar phase behaviour. This

was consistent with what has previously been reported for micelle formation and other liquid crystal phases in EAN, due to the higher solubility of hydrocarbons in EAN than in water.

In 2007, Han *et al.* reported the formation of microemulsions containing ILs dispersed in supercritical CO<sub>2</sub>.<sup>130</sup> The ILs trialled contained the 1,1,3,3-tetramethylguanidinium cation with either an acetate, lactate or trifluoroacetate anion. The IL in supercritical CO<sub>2</sub> systems were successfully used as a solvent system to prepare spherical gold nanoparticles or gold networks.<sup>130</sup>

A water-in-IL microemulsion containing BMIm PF<sub>6</sub> as the IL and TX-100 as the surfactant was reported by Zheng *et al.* in 2007 and used to prepare ZrO<sub>2</sub> nanoparticles.<sup>131</sup>

A complex and non-standard emulsion system with two IL-containing phases was recently reported by Friberg in 2007 using the IL BMIm BF<sub>4</sub> in both phases.<sup>132</sup> The first phase was a microemulsion of BMIm BF<sub>4</sub> in water stabilised by a non-ionic surfactant, and the second phase consisted of lamellar liquid crystals of the BMIm BF<sub>4</sub> and the same surfactant in water. The investigation was focussed on the algebraic treatment of the phase diagram for the effect of evaporation on the microemulsion. It was found that on evaporation the solvent phase containing the IL-in-water microemulsion went from a water-in-IL phase to a bicontinuous structure. The liquid crystal-in-water phase formed vesicles under high energy emulsification. When there was sufficient evaporation the two phases interacted, thus modifying each other. The maximum level of evaporation where the vesicles remained was determined relative to the IL concentration, and above this evaporation level the vesicles returned to a liquid crystal structure.<sup>132</sup>

In related studies, ILs have been used as surfactants to stabilise microemulsions. BMIm BF<sub>4</sub> was successfully used as an additive in an oil-in-water microemulsion to modify the droplets, leading to better separation of the test flavones analysed.<sup>133</sup> C<sub>16</sub>MIm Cl was used as a surfactant in the ternary system containing water and 1-decanol, forming lamellar and hexagonal phases,<sup>134</sup> and C<sub>8</sub>MIm Cl as a surfactant in water and alcohol ternary systems.<sup>135</sup> Similarly stable microemulsions containing water, methyl methacrylate and an IL as a surfactant were produced using the ILs C<sub>12</sub>MIm Br or 1-(2-acryloyloxyundecyl)-3-methylimidazolium bromide.<sup>136</sup> The second of these ILs was polymerisable and was successfully used to make polymer latexes with an average nanoparticle size of 30 nm. These microemulsions were also used to make gels and microporous structures.<sup>136</sup>

## 9. Emulsions containing ionic liquids

The earliest use of ILs in emulsions appears to have been by Merrigan *et al.* in 2000, where dispersions were prepared of perfluorohexane in the IL C<sub>6</sub>MIm PF<sub>6</sub> using fluorinated imidazolium ILs as surfactants.<sup>137</sup>

A diverse range of emulsions containing ILs was reported by Binks *et al.* in 2003 which were stabilised using silica nanoparticles.<sup>138</sup> This was a screening study which demonstrated the ability to make simple (*e.g.* IL-in-oil) and complex (*e.g.* IL-in-oil in water) emulsions containing ILs stabilised by silica nanoparticles. A range of imidazolium ILs were used

which were immiscible in water and/or the hydrophobic solvents. Many different solvent combinations were shown to lead to emulsions.<sup>138</sup>

An emulsion of toluene in BMIm PF<sub>6</sub> was reported by Kimizuka and Nakashima in 2003, and was successfully used to produce hollow titania microspheres.<sup>139</sup>

A few studies have used emulsion polymerisation with IL polymerisable monomers to make polymer beads which have been trialled successfully as catalyst supports<sup>140,141</sup> and as part of a biosensor.<sup>142</sup> These have not utilised the self-assembly capabilities of ILs, but only standard polymerisation and emulsion techniques.<sup>140–142</sup> Previous to the work on ILs, the molten salt of methyl ammonium ethane sulfonate was used in emulsions as the polar phase dispersed in a nonpolar liquid with a block copolymer emulsifier.<sup>143</sup> The nonpolar liquid and emulsifier could be polymerised to obtain droplets of the molten salt in polyurethane.<sup>143</sup>

## 10. Nanostructured materials generated in ionic liquid amphiphile self-assembly systems

The use of ILs in the preparation of inorganic materials is a rapidly progressing field.<sup>7,144,145</sup> The use of ILs in the preparation of nanostructured materials using self-assembly processes has mostly involved the use of amphiphilic ILs (AmILs) in water or other solvents, replacing traditional amphiphiles.<sup>146–155,157</sup> ILs have been widely used as structure-directing solvents,<sup>156–166</sup> and as ionothermal or solvothermal solvents,<sup>167–172</sup> in the preparation of nanostructures. In this section, the use of ILs as amphiphile self-assembly solvents for preparation of nanostructured materials is discussed. To date, this area has received limited attention in the literature.

In 2004–2005, Hao *et al.* reported a method to prepare semiconductor ZnS nanoparticles using amphiphile self-assembly in an IL,<sup>104</sup> along with the analogous method in water.<sup>173</sup> Amphiphile systems of zinc 2,2-dihydroperfluorooctanoate (Zn(OOCCH<sub>2</sub>C<sub>6</sub>F<sub>13</sub>)<sub>2</sub>) and tetradecyldimethylamine oxide (C<sub>14</sub>DMAO) were assembled in either BMIm BF<sub>4</sub> or BMIm PF<sub>6</sub> to form bilayer vesicles (described previously in section 7 of this review). Interestingly, vesicles formed in the ILs from the Zn amphiphile with or without the presence of C<sub>14</sub>DMAO, unlike in water, indicating a probable solvophobic interaction between the Zn amphiphile and the IL. ZnS nanoparticles were formed when H<sub>2</sub>S gas was flowed through the vesicle solution and were spherical or regular hexahedral in shape.

Microemulsions containing ILs as a solvent phase have successfully been used to prepare nanoparticles. The microemulsion of guanidinium ILs in supercritical CO<sub>2</sub> was used to prepare spherical gold nanoparticles or gold networks,<sup>130</sup> and BMIm PF<sub>6</sub> in water was used to prepare tetragonal ZrO<sub>2</sub> nanoparticles.<sup>131</sup>

The synthesis of hollow titania microspheres were reported by Kimizuka and Nakashima in 2003 from a toluene-in-IL emulsion.<sup>139</sup> This method was based on a technique reported by Schacht *et al.* in 1996 using the interface of an oil-in-water emulsion to prepare mesoporous silicas with macrostructure.<sup>174</sup> The method of Kimizuka and Nakashima involves toluene droplets containing the titania precursors being

dispersed in BMIm BF<sub>4</sub>. The hollow titania microspheres form at the interface, where it is believed that trace amounts of water (e.g. 0.1%) present in the IL are crucial for the sol-gel reaction. It was briefly mentioned that this technique was also used to prepare hollow microspheres from other metal oxides such as Zr, Hf, Nb and In, and that the IL C<sub>8</sub>MIm BF<sub>4</sub> also led to the formation of hollow microspheres.<sup>139</sup>

## 11. Conclusions and the future of ionic liquids as amphiphile self-assembly media

In this review, we have discussed the use of ionic liquids as solvents for the self-assembly of amphiphiles. It has been established that select ionic liquids can support the same types of amphiphile self-assembly phases as aqueous systems, though due to the greater solubility of hydrocarbons in ionic liquids, amphiphiles with longer hydrocarbon chains are frequently required to achieve similar phases under otherwise comparable conditions.

In the past few years, studies with ILs have markedly increased the number of solvents known to promote amphiphile self-assembly.<sup>61–63</sup> ILs are providing new systems to explore the factors governing amphiphile self-assembly and the formation of aggregate structures. For example, reports that AILs support amphiphile self-assembly are challenging the view that amphiphile self-assembly generally only occurs in solvents which can form multiple hydrogen bonds.<sup>53</sup>

A few templated nanostructured materials have been reported which utilise the ability of ILs to self-assemble amphiphiles. It is envisaged that this will represent a strong future growth area within the field of ILs and templated materials synthesis. Other potential applications for these ILs which utilise amphiphile self-assembly are in detergency/dry cleaning, dispersion, wetting, lubrication, protein crystallization, biocatalysis, separation, encapsulation and controlled release, and as micro-reactors for organic and inorganic synthesis.

## Abbreviations

IL	Ionic liquid
PIL	Protic ionic liquid
AIL	Aprotic ionic liquid
AmIL	Amphiphilic ionic liquid
LCP	Liquid crystal phase
EMIm	1-Ethyl-3-methylimidazolium
BMIm	1-Butyl-3-methylimidazolium
MOMIm	1-Methoxymethyl-3-methylimidazolium
EOMIm	1-(2-Methoxyethyl)-3-methylimidazolium
Tf <sub>2</sub> N	Bis(trifluoromethanesulfonyl)imide
TFA	Trifluoroacetate
EAN	Ethylammonium nitrate
EOAN	Ethanolammonium nitrate
MAF	Methylammonium formate
EAF	Ethylammonium formate
BAF	Butylammonium formate
PAF	Propylammonium formate
PeAF	Pentylammonium formate
2MPAF	2-Methylpropylammonium formate

(continued)

2MBAF	2-Methylbutylammonium formate
EOAF	Ethanolammonium formate
2POAF	2-Propanolammonium formate
EOAA	Ethanolammonium acetate
EAP	Ethylammonium propionate
EAB	Ethylammonium butyrate
EAG	Ethylammonium glycolate
EAL	Ethylammonium lactate
EOAL	Ethanolammonium lactate
EAHS	Ethylammonium hydrogen sulfate
DEAF	Diethylammonium formate
TEAF	Triethylammonium formate
DEOAF	Diethanolammonium formate
DMAF	Dimethylammonium formate
DMAHS	Dimethylammonium hydrogen sulfate
EOAHS	Ethanolammonium hydrogen sulfate
2MEAF	2-Methoxyethylammonium formate
22HEEAF	2-(2-Hydroxyethoxy)ethylammonium formate
22HEEAN	2-(2-Hydroxyethoxy)ethylammonium nitrate
TMGA	1,1,3,3-Tetramethylguanidinium acetate
TMGL	1,1,3,3-Tetramethylguanidinium lactate
TMGTFA	1,1,3,3-Tetramethylguanidinium trifluoroacetate
BF <sub>4</sub>	Tetrafluoroborate
PF <sub>6</sub>	Hexafluorophosphate
FA	Formamide
NMF	<i>N</i> -Methylformamide
DMF	<i>N,N'</i> -Dimethylformamide
NMA	<i>N</i> -Methylacetamide
DMA	<i>N,N'</i> -Dimethylacetamide
<i>N</i> -EtFOSA	<i>N</i> -Ethyl perfluorooctylsulfonamide
DMSO	Dimethyl sulfoxide
Tween 20	Polyoxyethylenesorbitan monooleate, C <sub>58</sub> H <sub>114</sub> O <sub>26</sub>
OBG	<i>n</i> -Octyl-β-D-glucopyranoside
AOT	Sodium bis(2-ethylhexyl) sulfosuccinate
SDS	Sodium dodecyl sulfate
docSS	Dioctyl sulfosuccinate
SB3-10	Sulfobetaine 10 or <i>n</i> -decyl- <i>N,N</i> -dimethyl-3-ammonio-1-propanesulfonate
C <sub>x</sub> TAB	Alkyl <sub>x</sub> trimethylammonium bromide
CTAB	C <sub>16</sub> TAB, hexadecyltrimethylammonium bromide
C <sub>x</sub> PyrB	Alkyl <sub>x</sub> pyridinium bromide
C <sub>x</sub> AN	Alkyl <sub>x</sub> ammonium nitrate
Brij 35	Polyoxyethylene 23 lauryl ether
Brij 76	Polyoxyethylene 10 stearyl ether
Brij 700	Polyoxyethylene 100 stearyl ether
TX-100	Triton X-100 or (CH <sub>3</sub> C(CH <sub>3</sub> ) <sub>2</sub> CH <sub>2</sub> C(CH <sub>3</sub> ) <sub>2</sub> -C <sub>6</sub> H <sub>4</sub> (OCH <sub>2</sub> CH <sub>2</sub> ) <sub>9,5</sub> OH)
P123	Pluronic P123 (EO <sub>20</sub> PO <sub>70</sub> EO <sub>20</sub> )
C <sub>n</sub> E <sub>m</sub>	Polyoxyethylene alkyl ether, C <sub>n</sub> H <sub>2n+1</sub> (OCH <sub>2</sub> CH <sub>2</sub> ) <sub>m</sub> OH
CetMe <sub>2</sub> BzNCl	Cetyldimethylbenzylammonium chloride
Glycolipid 1	2-(2,3,4,5,6-Pentahydroxyhexanoylamino)-pentanedioic acid diheptadecyl ester

(continued)

Glycolipid 2	2-(2,3,4,5,6-Pentahydroxyhexanoylamino)pentanedioic acid bis[(3-dodecyloxypropyl)amide]
DPPC	Dipalmitoylphosphatidylcholine
DPPE	Dipalmitoylphosphatidylethanolamine
DSPC	$\beta$ , $\gamma$ -Distearoylphosphatidylcholine
DLPC	Dilauroylphosphatidylcholine
DMPC	Dimyristoylphosphatidylcholine
DPPG	Dipalmitoylphosphatidylglycerol
DPPA	Dipalmitoylphosphatidic acid
Myv	Myverol 18-99K
Phyt	Phytantriol
L <sub>1</sub>	Micellar
I <sub>1</sub>	Discrete cubic
H <sub>1</sub>	Normal hexagonal
V <sub>1</sub>	Normal bicontinuous cubic
L <sub><math>\alpha</math></sub>	Lamellar
V <sub>2</sub>	Inverse bicontinuous cubic
H <sub>2</sub>	Inverse hexagonal
I <sub>2</sub>	Inverse discrete cubic
L <sub>2</sub>	Inverse micellar
L <sub><math>\beta</math></sub>	Partially ordered lamellar
L <sub><math>\beta'</math></sub>	Partially ordered lamellar
L <sub>C</sub>	Crystalline
P <sub><math>\beta'</math></sub>	Partially ordered two-dimensional oblique structure
T <sub>C</sub>	Cloud point

## Acknowledgements

C.J.D. is the recipient of an Australian Research Council (ARC) Federation Fellowship. This work was also partly supported by an ARC Discovery Project grant, DP0666961.

## References

1. T. L. Greaves and C. J. Drummond, *Chem. Rev.*, 2008, **108**, 206.
2. T. Welton, *Chem. Rev.*, 1999, **99**, 2071.
3. N. Jain, A. Kumar, S. Chauhan and S. M. S. Chauhan, *Tetrahedron*, 2005, **61**, 1015.
4. J. Muzart, *Adv. Synth. Catal.*, 2006, **348**, 275.
5. V. I. Parvulescu and C. Hardacre, *Chem. Rev.*, 2007, **107**, 2615.
6. F. Van Rantwijk and R. A. Sheldon, *Chem. Rev.*, 2007, **107**, 2757.
7. Y. Zhou, *Curr. Nanosci.*, 2005, **1**, 35.
8. C. F. Poole, *J. Chromatogr., A*, 2004, **1037**, 49.
9. J. F. Liu, J. A. Jonsson and G. B. Jiang, *TrAC, Trends Anal. Chem.*, 2005, **24**, 20.
10. S. Pandey, *Anal. Chim. Acta*, 2006, **556**, 38.
11. Z. Yang and W. B. Pan, *Enzyme Microb. Technol.*, 2005, **37**, 19.
12. H. Bloom and V. C. Reinsborough, *Aust. J. Chem.*, 1967, **20**, 2583.
13. H. Bloom and V. C. Reinsborough, *Aust. J. Chem.*, 1968, **21**, 1525.
14. V. C. Reinsborough and J. P. Valleeau, *Aust. J. Chem.*, 1968, **21**, 2905.
15. H. Bloom and V. C. Reinsborough, *Aust. J. Chem.*, 1969, **22**, 519.
16. V. C. Reinsborough, *Aust. J. Chem.*, 1970, **23**, 1473.
17. D. F. Evans, A. Yamauchi, R. Roman and E. Z. Casassa, *J. Colloid Interface Sci.*, 1982, **88**, 89.
18. D. F. Evans, A. Yamauchi, G. J. Wei and V. A. Bloomfield, *J. Phys. Chem.*, 1983, **87**, 3537.
19. A. Ray, *J. Am. Chem. Soc.*, 1969, **91**, 6511.
20. A. Ray, *Nature*, 1971, **231**, 313.
21. H. N. Singh, S. M. Saleem, R. P. Singh and K. S. Birdi, *J. Phys. Chem.*, 1980, **84**, 2191.
22. I. Rico and A. Lattes, *J. Phys. Chem.*, 1986, **90**, 5870.
23. X. Auvray, C. Petipas, R. Anthore, I. Rico, A. Lattes, A. A. Z. Samii and A. Desavignac, *Colloid Polym. Sci.*, 1987, **265**, 925.
24. A. Belmajdoub, K. Elbayed, J. Brondeau, D. Canet, I. Rico and A. Lattes, *J. Phys. Chem.*, 1988, **92**, 3569.
25. A. Lattes and I. Rico, *Colloids Surf.*, 1989, **35**, 221.
26. X. Auvray, C. Petipas, R. Anthore, I. Rico and A. Lattes, *J. Phys. Chem.*, 1989, **93**, 7458.
27. X. Auvray, T. Perche, R. Anthore, C. Petipas, I. Rico and A. Lattes, *Langmuir*, 1991, **7**, 2385.
28. X. Auvray, T. Perche, C. Petipas, R. Anthore, M. J. Marti, I. Rico and A. Lattes, *Langmuir*, 1992, **8**, 2671.
29. T. Perche, X. Auvray, C. Petipas, R. Anthore, E. Perez, I. Rico-Lattes and A. Lattes, *Langmuir*, 1996, **12**, 863.
30. M. S. Akhter and S. M. Alawi, *Colloids Surf., A*, 2000, **173**, 95.
31. M. S. Akhter and S. M. Alawi, *Colloids Surf., A*, 2003, **219**, 281.
32. X. Auvray, C. Petipas, T. Perche, R. Anthore, M. J. Marti, I. Rico and A. Lattes, *J. Phys. Chem.*, 1990, **94**, 8604.
33. A. J. Ward and C. du Reau, *Surfactant Association in Nonaqueous Media*, in *Surface and Colloid Science*, ed. E. Matijevic, Plenum Press, New York, 1993, ch 4, p. 15.
34. A. Belmajdoub, J. P. Marchal, D. Canet, I. Rico and A. Lattes, *New J. Chem.*, 1987, **11**, 415.
35. X. Auvray, C. Petipas, A. Lattes and I. Rico-Lattes, *Colloids Surf., A*, 1997, **123**, 247.
36. I. Rico and A. Lattes, *New J. Chem.*, 1984, **8**, 429.
37. X. Auvray, M. D. P. Abiyala, C. Petipas, I. Rico and A. Lattes, *Langmuir*, 1993, **9**, 444.
38. G. A. Baker and S. Pandey, *ACS Symp. Ser.*, 2005, **901**, 234.
39. J. Hao and T. Zemb, *Curr. Opin. Colloid Interface Sci.*, 2007, **12**, 129.
40. M. Antonietti, D. B. Kuang, B. Smarsly and Z. Yong, *Angew. Chem., Int. Ed.*, 2004, **43**, 4988.
41. K. Binnemans, *Chem. Rev.*, 2005, **105**, 4148.
42. C. Chiappe and D. Pieraccini, *J. Phys. Org. Chem.*, 2005, **18**, 275.
43. M. C. Buzzeo, R. G. Evans and R. G. Compton, *Chem-PhysChem*, 2004, **5**, 1106.
44. D. R. MacFarlane, J. M. Pringle, K. M. Johansson, S. A. Forsyth and M. Forsyth, *Chem. Commun.*, 2006, 1905.
45. B. Nuthakki, T. L. Greaves, I. Krodkiewska, A. Weerawardena, M. I. Burgar, R. J. Mulder and C. J. Drummond, *Aust. J. Chem.*, 2007, **60**, 21.
46. F. Kohler, H. Atrops, H. Kalall, E. Liebermann, E. Wilhelm, F. Ratkovic and T. Salamon, *J. Phys. Chem.*, 1981, **85**, 2520.
47. N. T. Southall, K. A. Dill and A. D. J. Haymet, *J. Phys. Chem. B*, 2002, **106**, 521.
48. D. Chandler, *Nature*, 2005, **437**, 640.
49. E. E. Meyer, K. J. Rosenberg and J. Israelachvili, *Proc. Natl. Acad. Sci. U. S. A.*, 2006, **103**, 15739.
50. S. B. Johnson, C. J. Drummond, P. J. Scales and S. Nishimura, *Langmuir*, 1995, **11**, 2367.
51. S. B. Johnson, C. J. Drummond, P. J. Scales and S. Nishimura, *Colloids Surf., A*, 1995, **103**, 195.
52. D. F. Evans, S.-H. Chen, G. W. Schriver and E. M. Arnett, *J. Am. Chem. Soc.*, 1981, **103**, 481.
53. D. F. Evans, *Langmuir*, 1988, **4**, 3.
54. R. F. Considine and C. J. Drummond, *Langmuir*, 2000, **16**, 631.
55. D. Mirejovsky and E. Arnett, *J. Am. Chem. Soc.*, 1983, **105**, 1112.
56. T. J. O'Leary and I. W. Levin, *J. Phys. Chem.*, 1984, **88**, 4074.
57. W. Tamuralis, L. J. Lis and P. J. Quinn, *J. Colloid Interface Sci.*, 1992, **150**, 200.
58. N. Kimizuka and T. Nakashima, *Langmuir*, 2001, **17**, 6759.
59. T. Nakashima and N. Kimizuka, *Chem. Lett.*, 2002, **31**, 1018.
60. J. Tang, D. Li, C. Sun, L. Zheng and J. Li, *Colloids Surf., A*, 2006, **273**, 24.
61. T. L. Greaves, A. Weerawardena, C. Fong and C. J. Drummond, *Langmuir*, 2007, **23**, 402.
62. T. L. Greaves, A. Weerawardena, C. Fong and C. J. Drummond, *J. Phys. Chem. B*, 2007, **111**, 4082.
63. T. L. Greaves, A. Weerawardena, I. Krodkiewska and C. J. Drummond, *J. Phys. Chem. B*, 2008, **112**, 896.



64. A. H. Beesley, D. F. Evans and R. G. Laughlin, *J. Phys. Chem.*, 1988, **92**, 791.
65. W. Martino, J. F. De La Mora, Y. Yoshida, G. Saito and J. Wilkes, *Green Chem.*, 2006, **8**, 390.
66. H. Tokuda, K. Hayamizu, K. Ishii, M. A. B. H. Susan and M. Watanabe, *J. Phys. Chem. B*, 2005, **109**, 6103.
67. J. G. Huddleston, A. E. Visser, W. M. Reichert, H. D. Willauer, G. A. Broker and R. D. Rogers, *Green Chem.*, 2001, **3**, 156.
68. L. Berthon, S. I. Nikitenko, I. Bisel, C. Berthon, M. Faucon, B. Saucerotte, N. Zorz and P. Moisy, *Dalton Trans.*, 2006, 2526.
69. J. N. Israelachvili, D. J. Mitchell and B. W. Ninham, *J. Chem. Soc., Faraday Trans. 2*, 1976, **72**, 1525.
70. T. Kaasgaard and C. J. Drummond, *Phys. Chem. Chem. Phys.*, 2006, **8**, 4957.
71. S. T. Hyde, Identification of Lyotropic Liquid Crystalline Mesophases, in *Handbook of Applied Surface and Colloid Chemistry*, ed. K. Holmberg, John Wiley & Sons Ltd, New York, 2001, ch. 16.
72. C. J. Drummond, F. Grieser and T. W. Healy, *Chem. Phys. Lett.*, 1987, **140**, 493.
73. J. Kibblewhite, C. J. Drummond, F. Grieser and T. W. Healy, *J. Phys. Chem.*, 1987, **91**, 4658.
74. A. C. F. Ribeiro, V. M. M. Lobo, A. J. M. Valente, E. F. G. Azevedo, M. D. Miguel and H. D. Burrows, *Colloid Polym. Sci.*, 2004, **283**, 277.
75. J. Mata, D. Varade and P. Bahadur, *Thermochim. Acta*, 2005, **428**, 147.
76. K. A. Fletcher and S. Pandey, *Langmuir*, 2004, **20**, 33.
77. J. Škerjanc, K. Kogel and J. Cerar, *Langmuir*, 1999, **15**, 5023.
78. A. Gonzalez-Perez, L. M. Varela, M. Garcia and J. R. Rodriguez, *J. Colloid Interface Sci.*, 2006, **293**, 213.
79. S. B. Velasco, M. Turmine, D. Di Caprio and P. Letellier, *Colloids Surf., A*, 2006, **275**, 50.
80. J. L. Anderson, V. Pino, E. C. Hagberg, V. V. Sheares and D. W. Armstrong, *Chem. Commun.*, 2003, 2444.
81. C. D. Tran and S. F. Yu, *J. Colloid Interface Sci.*, 2005, **283**, 613.
82. S. Thomaier and W. Kunz, *J. Mol. Liq.*, 2007, **130**, 104.
83. C. Patrascu, F. Gauffre, F. Nallet, R. Bordes, J. Oberdisse, N. de Lauth-Viguerie and C. Mingotaud, *ChemPhysChem*, 2006, **7**, 99.
84. C. J. Drummond, G. G. Warr, F. Grieser, B. W. Ninham and D. F. Evans, *J. Phys. Chem.*, 1985, **89**, 2103.
85. D. F. Evans, E. W. Kaler and W. J. Benton, *J. Phys. Chem.*, 1983, **87**, 533.
86. M. U. Araos and G. G. Warr, *J. Phys. Chem. B*, 2005, **109**, 14275.
87. R. Atkin and G. G. Warr, *J. Am. Chem. Soc.*, 2005, **127**, 11940.
88. D. Seth, A. Chakraborty, P. Setua and N. Sarkar, *J. Phys. Chem. B*, 2007, **111**, 4781.
89. Y. He, Z. Li, P. Simone and T. P. Lodge, *J. Am. Chem. Soc.*, 2006, **128**, 2745.
90. P. M. Simone and T. P. Lodge, *Macromolecules*, 2008, **41**, 1753.
91. P. M. Simone and T. P. Lodge, *Macromol. Chem. Phys.*, 2007, **208**, 339.
92. Y. Y. He, P. G. Boswell, P. Buhlmann and T. P. Lodge, *J. Phys. Chem. B*, 2007, **111**, 4645.
93. Y. Y. He and T. P. Lodge, *Chem. Commun.*, 2007, 2732.
94. W. Tamura-Lis and L. J. Lis, *J. Phys. Chem.*, 1987, **91**, 4625.
95. W. Tamura-Lis, L. J. Lis and P. J. Quinn, *Biophys. J.*, 1988, **53**, 489.
96. L. Y. Wang, X. Chen, Y. C. Chai, J. C. Hao, Z. M. Sui, W. C. Zhuang and Z. W. Sun, *Chem. Commun.*, 2004, 2840.
97. D. J. Mitchell, G. J. T. Tiddy, L. Waring, T. Bostock and M. P. McDonald, *J. Chem. Soc., Faraday Trans. 1*, 1983, **79**, 975.
98. T. Wolff and G. von Bunau, *Ber. Bunsen-Ges. Phys. Chem.*, 1984, **88**, 1098.
99. T. Warnheim and A. Jonsson, *J. Colloid Interface Sci.*, 1988, **125**, 627.
100. J. Clogston, J. Rathman, D. Tomasko, H. Walker and M. Caffrey, *Chem. Phys. Lipids*, 2000, **107**, 191.
101. S. T. Hyde and S. Andersson, *Z. Kristallogr.*, 1984, **168**, 213.
102. J. Barauskas and T. Landh, *Langmuir*, 2003, **19**, 9562.
103. R. P. Swatloski, S. K. Spear, J. D. Holbrey and R. D. Rogers, *J. Am. Chem. Soc.*, 2002, **124**, 4974.
104. J. C. Hao, A. X. Song, J. Z. Wang, X. Chen, W. C. Zhuang, F. Shi, F. Zhou and W. M. Liu, *Chem.–Eur. J.*, 2005, **11**, 3936.
105. M. Yoshio, T. Mukai, K. Kanie, M. Yoshizawa, H. Ohno and T. Kato, *Chem. Lett.*, 2002, **31**, 320.
106. M. Yoshio, T. Mukai, K. Kanie, M. Yoshizawa, H. Ohno and T. Kato, *Adv. Mater.*, 2002, **14**, 351.
107. I. Rico and A. Lattes, *J. Colloid Interface Sci.*, 1984, **102**, 285.
108. S. Friberg and M. Podzimek, *Colloid Polym. Sci.*, 1984, **262**, 252.
109. J. Eastoe, M. J. Hollamby and L. Hudson, *Adv. Colloid Interface Sci.*, 2006, **128**, 5.
110. H. S. Xia, J. Yu, Y. Y. Jiang, I. Mahmood and H. Z. Liu, *Ind. Eng. Chem. Res.*, 2007, **46**, 2112.
111. H. X. Gao, J. C. Li, B. X. Han, W. N. Chen, J. L. Zhang, R. Zhang and D. D. Yan, *Phys. Chem. Chem. Phys.*, 2004, **6**, 2914.
112. Y. N. Gao, S. B. Han, B. X. Han, G. Z. Li, D. Shen, Z. H. Li, J. M. Du, W. G. Hou and G. Y. Zhang, *Langmuir*, 2005, **21**, 5681.
113. J. C. Li, J. L. Zhang, H. X. Gao, B. X. Han and L. Gao, *Colloid Polym. Sci.*, 2005, **283**, 1371.
114. Y. N. Gao, S. Q. Wang, L. Q. Zheng, S. B. Han, X. Zhang, D. M. Lu, L. Yu, Y. Q. Ji and G. Y. Zhang, *J. Colloid Interface Sci.*, 2006, **301**, 612.
115. Y. Gao, J. Zhang, H. Y. Xu, X. Y. Zhao, L. Q. Zheng, X. W. Li and L. Yu, *ChemPhysChem*, 2006, **7**, 1554.
116. Y. Gao, N. Li, L. Q. Zheng, X. Y. Zhao, S. H. Zhang, B. X. Han, W. G. Hou and G. Z. Li, *Green Chem.*, 2006, **8**, 43.
117. Y. Gao, N. Li, L. Q. Zheng, X. Y. Zhao, J. Zhang, Q. Cao, M. W. Zhao, Z. Li and G. Y. Zhang, *Chem.–Eur. J.*, 2007, **13**, 2661.
118. Y. Gao, N. Li, L. Q. Zheng, X. T. Bai, L. Yu, X. Y. Zhao, J. Zhang, M. W. Zhao and Z. Li, *J. Phys. Chem. B*, 2007, **111**, 2506.
119. N. Li, Y. A. Gao, L. Q. Zheng, J. Zhang, L. Yu and X. W. Li, *Langmuir*, 2007, **23**, 1091.
120. J. Eastoe, S. Gold, S. E. Rogers, A. Paul, T. Welton, R. K. Heenan and I. Grillo, *J. Am. Chem. Soc.*, 2005, **127**, 7302.
121. D. Chakraborty, D. Seth, A. Chakraborty and N. Sarkar, *J. Phys. Chem. B*, 2005, **109**, 5753.
122. D. R. Chang, *Langmuir*, 1990, **6**, 1132.
123. S. Q. Cheng, X. G. Fu, J. H. Liu, J. L. Zhang, Z. F. Zhang, Y. L. Wei and B. X. Han, *Colloids Surf., A*, 2007, **302**, 211.
124. D.-M. Zhu, K.-I. Feng and Z. A. Schelly, *J. Phys. Chem.*, 1992, **96**, 2382.
125. D. Seth, A. Chakraborty, P. Setua and N. Sarkar, *J. Chem. Phys.*, 2007, **126**, 224512.
126. D. Seth, A. Chakraborty, P. Setua and N. Sarkar, *Langmuir*, 2006, **22**, 7768.
127. K. Behera, P. Dahiya and S. Pandey, *J. Colloid Interface Sci.*, 2007, **307**, 235.
128. S. Q. Cheng, J. L. Zhang, Z. F. Zhang and B. X. Han, *Chem. Commun.*, 2007, 2497.
129. R. Atkin and G. G. Warr, *J. Phys. Chem. B*, 2007, **111**, 9309.
130. J. H. Liu, S. Q. Cheng, J. L. Zhang, X. Y. Feng, X. G. Fu and B. X. Han, *Angew. Chem., Int. Ed.*, 2007, **46**, 3313.
131. N. Li, B. Dong, W. L. Yuan, Y. Gao, L. Q. Zheng, Y. M. Huang and S. L. Wang, *J. Dispersion Sci. Technol.*, 2007, **28**, 1030.
132. S. E. Friberg, *J. Colloid Interface Sci.*, 2007, **307**, 494.
133. H. G. Zhang, K. Tian, J. H. Tang, S. D. Qi, H. L. Chen, X. G. Chen and Z. D. Hu, *J. Chromatogr., A*, 2006, **1129**, 304.
134. G. D. Zhang, X. A. Chen, Y. Z. Xie, Y. R. Zhao and H. Y. Qiu, *J. Colloid Interface Sci.*, 2007, **315**, 601.
135. G. D. Zhang, X. Chen, Y. R. Zhao, Y. Z. Xie and H. Y. Qiu, *J. Phys. Chem. B*, 2007, **111**, 11708.
136. F. Yan and J. Texter, *Chem. Commun.*, 2006, 2696.
137. T. L. Merrigan, E. D. Bates, S. C. Dorman and J. H. Davis, *Chem. Commun.*, 2000, 2051.
138. B. P. Binks, A. K. F. Dyab and P. D. I. Fletcher, *Chem. Commun.*, 2003, 2540.
139. T. Nakashima and N. Kimizuka, *J. Am. Chem. Soc.*, 2003, **125**, 6386.
140. M. J. Muldoon and C. M. Gordon, *J. Polym. Sci., Part A: Polym. Chem.*, 2004, **42**, 3865.
141. M. S. P. Lopez, D. Mecerreyes, E. Lopez-Cabarcos and B. Lopez-Ruiz, *Biosens. Bioelectron.*, 2006, **21**, 2320.
142. R. Marcilla, M. Sanchez-Paniagua, B. Lopez-Ruiz, E. Lopez-Cabarcos, E. Ochoateca, H. Grande and D. Mecerreyes, *J. Polym. Sci., Part A: Polym. Chem.*, 2006, **44**, 3958.

143. M. H. Litt, C. S. Lin and I. M. Krieger, *J. Polym. Sci., Part A: Polym. Chem.*, 1990, **28**, 2777.
144. W. M. Reichert, J. D. Holbrey, K. B. Vigour, T. D. Morgan, G. A. Broker and R. D. Rogers, *Chem. Commun.*, 2006, 4767.
145. A. Taubert and Z. Li, *Dalton Trans.*, 2007, 723.
146. Y. Zhou and M. Antonietti, *Adv. Mater.*, 2003, **15**, 1452.
147. Y. Zhou and M. Antonietti, *Chem. Commun.*, 2003, 2564.
148. Y. Zhou and M. Antonietti, *Chem. Mater.*, 2004, **16**, 544.
149. A. Taubert, *Angew. Chem., Int. Ed.*, 2004, **43**, 5380.
150. M. A. Firestone, M. L. Dietz, S. Seifert, S. Trasobares, D. J. Miller and N. J. Zaluzec, *Small*, 2005, **1**, 754.
151. T. Brezesinski, C. Erpen, K.-I. Iimura and B. Smarsly, *Chem. Mater.*, 2005, **17**, 1683.
152. O. Sel, D. Kuang, M. Thommes and B. Smarsly, *Langmuir*, 2006, **22**, 2311.
153. A. M. Guloy, R. Ramlau, Z. J. Tang, W. Schnelle, M. Baitinger and Y. Grin, *Nature*, 2006, **443**, 320.
154. X. Y. Yu, C. H. Liu, J. G. Yang, H. H. Wu, P. Wu and M. Y. He, *Chin. J. Chem.*, 2006, **24**, 1282.
155. H. Park, S. H. Yang, Y. S. Jun, W. H. Hong and J. K. Kang, *Chem. Mater.*, 2007, **19**, 535.
156. Y. Zhou and M. Antonietti, *J. Am. Chem. Soc.*, 2003, **125**, 14960.
157. Z. Y. Li, H. T. Liu, Y. Liu, P. He and J. H. Li, *J. Phys. Chem. B*, 2004, **108**, 17512.
158. Y. J. Zhu, W. W. Wang, R. J. Qi and X. L. Hu, *Angew. Chem., Int. Ed.*, 2004, **43**, 1410.
159. E. R. Cooper, C. D. Andrews, P. S. Wheatley, P. B. Webb, P. Wormald and R. E. Morris, *Nature*, 2004, **430**, 1012.
160. Z. H. Li, Z. M. Liu, J. L. Zhang, B. X. Han, J. M. Du, Y. N. Gao and T. Jiang, *J. Phys. Chem. B*, 2005, **109**, 14445.
161. Y. Liu, M. J. Wang, Z. Y. Li, H. T. Liu, P. He and J. H. Li, *Langmuir*, 2005, **21**, 1618.
162. K. S. Yoo, T. G. Lee and J. Kim, *Microporous Mesoporous Mater.*, 2005, **84**, 211.
163. H. Choi, Y. J. Kim, R. S. Varma and D. D. Dionysiou, *Chem. Mater.*, 2006, **18**, 5377.
164. T. Hogben, R. E. Douthwaite, L. J. Gillie and A. C. Whitwood, *CrystEngComm*, 2006, **8**, 866.
165. N. S. Venkataramanan, K. Matsui, H. Kawanami and Y. Ikushima, *Green Chem.*, 2007, **9**, 18.
166. G. B. Hix, A. Turner, L. Vahter and B. M. Kariuki, *Microporous Mesoporous Mater.*, 2007, **99**, 62.
167. K. Jin, X. Y. Huang, L. Pang, J. Li, A. Appel and S. Wherland, *Chem. Commun.*, 2002, 2872.
168. D. N. Dybtsev, H. Chun and K. Kim, *Chem. Commun.*, 2004, 1594.
169. H. G. Zhu, J. F. Huang, Z. W. Pan and S. Dai, *Chem. Mater.*, 2006, **18**, 4473.
170. J. H. Liao and W. C. Huang, *Inorg. Chem. Commun.*, 2006, **9**, 1227.
171. E. R. Parnham, A. M. Z. Slawin and R. E. Morris, *J. Solid State Chem.*, 2007, **180**, 49.
172. Z. J. Lin, A. M. Z. Slawin and R. E. Morris, *J. Am. Chem. Soc.*, 2007, **129**, 4880.
173. J. Hao, J. Wang, W. Liu, R. Abdel-Rahem and H. Hoffmann, *J. Phys. Chem. B*, 2004, **108**, 1168.
174. S. Schacht, Q. Huo, I. G. Voigt-Martin, G. D. Stucky and F. Schüth, *Science*, 1996, **273**, 768.